CHALMERS
UNIVERSITY OF TECHNOLOGY

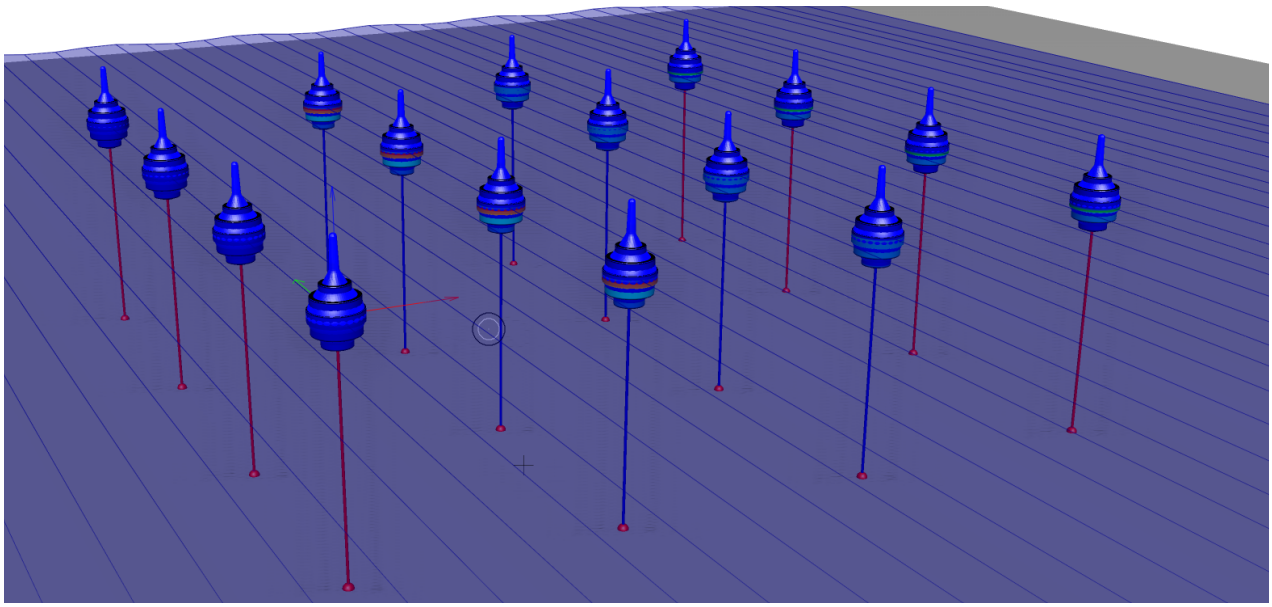

Assessment of interaction effects between wave energy converters

Master's thesis in the International Master's Programme in Mobility Engineering – Marine Technology

HRISHIKESH NITIN KHEDKAR

UDAY RAJDEEP SAKLESHPUR LOKESH GOWDA

DEPARTMENT OF MECHANICS AND MARITIME SCIENCES

CHALMERS UNIVERSITY OF TECHNOLOGY
Gothenburg, Sweden 2023
www.chalmers.se

MASTER'S THESIS IN THE INTERNATIONAL MASTER'S PROGRAMME
MOBILITY ENGINEERING – MARINE TECHNOLOGY

Assessment of interaction effects between wave energy converters

HRISHIKESH NITIN KHEDKAR and
UDAY RAJDEEP SAKLESHPUR LOKESH GOWDA

Department of Mechanics and Maritime Sciences
Division of Marine Technology

CHALMERS UNIVERSITY OF TECHNOLOGY
Göteborg, Sweden 2023

Assessment of interaction effects between wave energy converters

HRISHIKESH NITIN KHEDKAR and
UDAY RAJDEEP SAKLESHPUR LOKESH GOWDA

Master's Thesis
Department of Mechanics and Maritime Sciences
Division of Marine Technology
Chalmers University of Technology
SE-412 96 Göteborg
Sweden
Telephone: + 46 (0)31-772 1000

Cover:
The figure shows the modelled WECs in an array of a 4x4 layout developed using SIMA software.

Department of Mechanics and Maritime Sciences
Göteborg, Sweden

Assessment of interaction effects between wave energy converters

Master's thesis in the International Master's Programme in Mobility Engineering – Marine Technology

HRISHIKESH NITIN KHEDKAR and
UDAY RAJDEEP SAKLESHPUR LOKESH GOWDA

Department of Mechanics and Maritime Sciences
Division of Marine Technology
Chalmers University of Technology

Abstract

Wave energy is one of the abundant renewable energy sources in nature. The technology to harness wave energy is at technology readiness level TRL 7-8 (stage 4), i.e., single full-scale prototypes have been tested at sea according to the development steps defined by the European Marine Energy Centre. The next development goal is the wave park, in other words an array of wave energy converters (WECs). This thesis focuses on C4, the heaving point absorber WEC developed with the specifications from CorPower Ocean, and how it should be arranged in wave parks to maximize the harnessing of wave energy.

While it is important to improve the efficiency of the WEC, such a system is better utilized in groups forming an array of WECs, hence it is important to study the behaviour of such an array. One of the key challenges in modelling a WEC array (a.k.a. wave park) is the interaction effects between the WECs. Studies have shown that interaction effects between WECs are important to optimize the power output of the wave park. The aim of this thesis is to model two different WEC arrays of 16 WECs, grouped as 4x4 and 8x2 WECs, and study the interaction effects for different environmental conditions. The study investigates the characteristics of the two arrays by varying the distance between the WECs, the variation of the damping coefficient of the power take off (PTO) system for different environmental conditions.

A coupled hydrodynamic and structural response analysis is carried out using the DNV software SESAM. The power absorbed for all simulated conditions are evaluated and a methodology is proposed for the preliminary design analysis of wave parks.

From this study, it is concluded that the interaction effects play a significant role in the performance of the WECs. The power produced from wave parks depends on several factors and they must be systematically included in preliminary design studies. The optimization of the WEC array also depends on limiting the parameters to installation location. The methodology used in this study proved to be a good tool that incorporated both interaction effects and the design parameters. Examining these behaviours is crucial to unlocking and optimizing the full potential of wave parks.

Keywords: array, heaving point absorber, power absorption, wave energy converter, wave energy parks, wave interaction effects.

Contents

Preface

This thesis is a part of the international master's programme in Mobility Engineering's requirement for a master's degree at Chalmers University of Technology. It is also a part of the ongoing research project concerning the development of a wave energy park. The thesis project was carried out at the Division of Marine Technology, Department of Mechanics and Maritime Sciences, Chalmers University of Technology between January and August 2023.

We would like to thank our supervisor and examiner for this thesis, Professor Jonas W. Ringsberg, for inviting us to this interesting and exciting research project. We would also like to thank him for his endless support, feedback and guidance that helped us through this thesis project.

We would like to thank the co-supervisors Xinyuan Shao and Hua-Dong Yao for their guidance throughout the thesis, particularly Xinyuan's expertise in this research, modelling, and simulation procedures. Her kind advice, time and support given to us during the entire process guided us throughout this thesis.

We would like to thank CorPower for this research topic and their expertise. The discussions with them in certain aspects of the thesis proved helpful and is a valuable part of our thesis.

Finally, we would like to thank our families and friends for their endless love and support.

Göteborg, 2023-09-12

HRISHIKESH NITIN KHEDKAR and
UDAY RAJDEEP SAKLESHPUR LOKESH GOWDA

Nomenclature

List of acronyms

CoG	Centre of Gravity
FEM	Finite Element Method
IRH	Irregular High
IRHA	Irregular High Wave Angle
IRHL	Irregular High Layout
IRHW	Irregular High Water Depth
IRL	Irregular low
IRLA	Irregular Low Wave Angle
IRLL	Irregular Low Layout
IRLW	Irregular Low Water Depth
IRM	Irregular Medium
JONSWAP	Joint North Sea Wave Project
LCoE	Levelized Cost of Energy
PTO	Power Take Off
RH	Regular High
RL	Regular Low
TRL	Technology Readiness Level
WAB	Wave Activated Bodies
WEC	Wave Energy Converter

Roman notations

$\ddot{x}$	Acceleration	[m/s^2]
z	Buoy vertical position	[m]
z_{es}	End stop distance	[m]
F_{es}	End stop force	[N]
c	End stop force parameter	[-]
n	End stop force parameter	[-]
(X, Y, Z)	Global coordinates	[m]
$u\,(\cdot)$	Heave side step function	[-]
R_{loss}	Linear loss Damping	[kNs/m]
(x, y, z)	Local coordinates	[m]

P_a	PTO averaged power	[kW]
C_{PTO}	PTO Damping	[kNs/m]
P	PTO Power Output	[kW]
$\dot{Z_{rel}}$	Relative heave velocity	[m/s]
R_u	Useful Damping	[kNs/m]

Greek notation

g	Non-dimensional peak enhancement factor for JONSWAP spectrum	[-]

List of symbols and unit abbreviations

deg	Degrees
kg	Kilograms
kW	Kilowatt
MWh	Megawatt hour
m	Meter
N	Newton
s	Seconds

1 Introduction

This chapter presents the background and motivation of the study followed by the objectives derived from the motivation and the methodology used to achieve the objectives.

1.1 Background and motivation of study

Humans have evolved from self-sustenance to harnessing energy from the nature. In the present time, the energy demand by the society is higher than any time observed in the history of mankind. This demand must be met by utilizing various sources available in the nature. The usage of energy in the present, predicts the demand for it in the future. Several factors such as population, urbanization, and industrialization influence the rise in energy demand (Hasanuzzaman et al., 2020). The energy needed to meet this demand can be obtained by sources in nature that are broadly classified as renewable and non-renewable energies.

The major source of energy used by most of the population on the Earth is from fossil fuels formed over millions of years ago. This energy source is responsible for the increase in the carbon emissions. Therefore, it is a serious threat to the environment resulting in climate change (Güney, 2019). To reduce these effects and safeguard the environment, several countries have committed to reaching net zero carbon emissions by the year 2050 and one such way to be fossil free is by switching over to the renewable sources of energy such as wind, solar and tidal energy (Guo et al., 2022). Among all the renewable sources of energy, the wave energy and tidal energy are the most abundant and reliable source, offering advantages such as high energy density, low level of negative environmental impact and predictability (Sasaki, 2017). The technology to harness the wave energy is still not mature for commercial large-scale applications. Nevertheless, the European Commission has reached a provisional agreement in the renewable energy directive to have at least 42.5% renewable energy in the EU energy mix by the year 2030 and aiming to further increase the target to 45% for the same target year (EU, 2023).

There are several ways to harness wave energy using wave energy converters (WECs) (Aderinto and Li, 2019). They have different designs coming from different technology development companies that try to find an ideal design to absorb the maximum energy from the waves. Many unit systems are being tested worldwide with different Technology Readiness Levels (TRL) (EMEC, 2023) for their performance, for example, CorPower (CorPower Ocean, 2023), Waves4Power (Waves4Power, 2023), GEPS Techno (GEPS Techno, 2023), Bombora wave power (Bombora, 2023) and Wave Dragon (Wave Dragon, 2023) . The WECs have different designs and operating principles, there is no standard design that is considered being the most promising. They are classified based on their operating principle, location, power take off (PTO) system and directional characteristics (Czech and Bauer, 2012).

Based on the operating principle, the WECs are classified as oscillating water column, overtopping device and wave activated bodies (WABs) (Falcão, 2010; Drew et al., 2009).

- The oscillating water column WEC works by generating bidirectional airflow through a turbine. The water chamber has an opening under the water surface which allows the sea water to enter the chamber. The water level changes with

the wave amplitude and the air inside the chamber compresses and expands. This causes the air to flow in and out of the chamber through a turbine which generates electricity (Previsic, 2005).

- The overtopping device captures waves over the top of the WEC in a reservoir and it is allowed to flow to the sea through low head turbines which generate electricity (Polinder and Scuotto, 2005).
- The wave activated bodies oscillate with the wave motions in relation with another body part or a fixed point. The WEC motions are mainly heave, pitch and roll and these motions are used to produce electricity (Harris et al., 2004).

The directional characteristics of the WEC also influence the operation principle. The point absorbers are indifferent to the wave propagation direction while the attenuators need to be parallel to the wave propagation direction (Czech and Bauer, 2012). The PTO systems are generally using a Wells turbine, an impulse turbine, hydraulic systems, or a linear generator.

The WECs are currently deployed as a single unit in the ocean and studies are being conducted to evaluate their performance. The large commercialization requires these units to be deployed as an array of WEC's called wave energy park (Ruehl et al., 2012). There are many challenges to reach commercialization. The single unit systems are on TRL 7-8 (stage 4) as defined in the development steps for wave and tidal energy systems by the European marine energy centre (EMEC, 2023). However, wave energy parks have additional challenges. The interaction between the WEC's is one of the key challenges that must be fully understood and controlled (Babarit, 2013). The wave park design influences the fatigue life of mooring lines and power cables. Therefore the fatigue life is important to the lifecycle analysis (Yang et al., 2020). The Levelized Cost of Energy (LCoE), defined as the ratio of total annualized cost of the system to the total electrical load served, depends on the life cycle of the system. There is always a trade-off between LCoE and fatigue life of the array farm. Having a large array or a cluster of smaller arrays depends on these factors (Ringsberg et al., 2020). Interaction effects also influence the fatigue damage accumulation. This will significantly affect the maintenance and the cost for energy absorbed.

In the remaining text of this thesis, the following terminology and terms are used: "WEC model" includes the components of a single WEC unit i.e., mooring system, WEC buoy and the PTO system that is modelled for energy absorption; the "WEC buoy" refers to the heaving buoy that responds to waves and produces heave and other motions; and "array model" refers to the complete WEC array. In addition, the thesis focuses on the interaction effects and their impact on power production from WEC arrays, and the thesis has used CorPower's WEC as the study case. Figure 1-1 shows a schematic of interaction effects with two interaction-related wave components, radiated and diffracted wave, which are considered in the thesis.

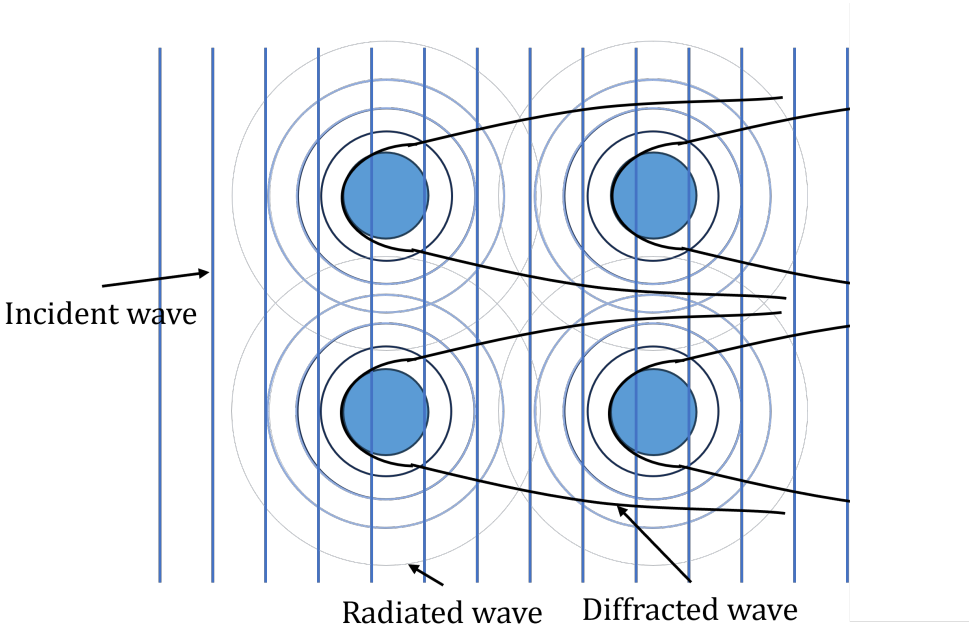

Figure 1-1: Schematic of two wave interaction effects.

In the study by Borgarino et al. (2012), the impact of wave interactions in large arrays was investigated. Two types of WECs were considered in the study, a heaving cylinder, and a surging barge. The study suggested several points related to interaction effects and array design optimisation. First, to increase the overall efficiency, selecting large-banded WECs resulted in positive wave interactions across a significant range of wave periods. Second, PTO damping values based on yearly energy production were preferred rather than the resonant frequency. This resulted in large damping values that limited the radiation effects. Furthermore, it was observed that WECs with higher efficiency are not suitable for the use of square arrays as they exhibit strong destructive interaction effects (masking effect). An exception arises wherein the square-based arrays perform better when the WECs are axisymmetric. This circumstance finds relevance in the CorPower WEC and the array studied in this thesis.

Yang et al. (2020) investigated the hydrodynamic interactions of WECs in two different array configurations using Waves4Power (Waves4Power, 2023) WEC buoy. The study used two types of mooring configurations as reference WEC systems, a 3-Moor WEC system, and a 2-Moor WEC system. Two 2-WEC simulation models and an additional 10-WEC simulation model were analysed using the fore-mentioned reference WEC systems. The 2-WEC simulation model without the mechanical coupling between the moorings were designed to capture the hydrodynamic interaction effects. The study showed that, power interaction factor values were near unity (1) for the simulated load cases with a minor difference of 0.01% when compared with both mooring alternatives. It was also observed that the interaction effects are more pronounced at shorter separating distances and smaller at longer separation distances. Additionally, this study confirmed the effects of mooring restraints at higher energy sea states and the significance of using fully coupled time domain simulations that takes mooring effects into account. Furthermore, one of the 10-WEC simulation model LessIsMoor (Ringsberg et al., 2020) showed the influence of wave direction with a positive gain of 5% in a smart array orientation and a loss of 7% in the performance of the array in a non-favourable orientation. These results are particularly interesting for the array configuration studied in this thesis. Although the mooring configuration is different from the ones studied by Yang et al. (2020), a similar effect of mooring on the power absorption can be expected.

1.2 Objectives

The main objective of this thesis is to study interaction effects between WECs using CorPower's point absorber WEC technology (CorPower Ocean, 2023) numerically when installed in different WEC arrays. The performance of the WEC arrays is analysed and compared with a base model, i.e., a numerical model without interaction effects. The numerical simulations help to study a wide variety of simulation parameters in a short period of time, whereas physical experiments would have been time-consuming, expensive, and limited to the capabilities of the test rig. In the thesis, the array models are made for two configurations presented in Section 3.2.

The main objective is divided into smaller goals:

1. Study the numerical single WEC model, with parametric sensitivity analysis on the design parameters of the PTO system and the environmental loads.
2. Verify the single WEC system results, namely resonance, with the values from the physical model.
3. Compare the effects of array design parameters such as water depth, array configuration, WEC separation distance, and array orientation with parametric sensitivity analysis on environmental loads.
4. Analyse the power production of the WEC array compared with the alternative cases in the identical environmental load parameters.
5. Analyse the interaction effects compared with the reference cases in similar environmental load parameters.

1.3 Limitations and assumptions

The thesis is part of the INTERACT project (2020) funded by the Swedish Energy Agency. The reference single WEC point absorber considered for this project is designed by CorPower (CorPower Ocean, 2023). The numerical model of this WEC has not been developed by the authors of this thesis. It was originally developed by PhD student Xinyuan Shao working and funded by the INTERACT project. It follows the simulation proposed by Yang et al. (2016) using fully-coupled simulations in the time domain using the DNV software SESAM (DNV GL, 2019b).

The following limitations and assumptions have been made in the study:

- The PTO system used for this thesis considers different damping coefficient for each sea states simulated. However, it is simplified as linear damping coefficient for that sea state and does not contain control system to optimize it at each instant of the WEC motion.
- The WECs are assumed to be installed on the coastal areas with a water depth of 46 meters and 55 meters. This is the region where the tides and currents are significant. These conditions are not considered in this thesis to limit the number of simulations.
- The main motion of the wave energy converters is generated from the wave energy and the resonance frequency is important to achieve maximum motion in heave that leads to highest power output. However, the resonance causes the response to be unpredictable and damaging to the WEC system, Hence, an additional control of PTO though coupling forces must be utilized to minimize this effect. This coupling force adds to the structural response of the WEC system.

- Biofouling is not considered because of the thesis's time constraint. It is proven to have a negative impact on the power absorption, lifecycle, and fatigue damage (Yang et al., 2017).
- No measurements on a single WEC or wave park were available. Hence, the work is purely numerical. Any validation of this data is not possible with the physical system. With the simulation data, the results from array configurations are weighed against each other for the power performance analysis.

1.4 Outline of the thesis

The thesis is composed of seven chapters. Chapter 1 presents the research background and the motivation for the current study. Chapter 2 explains the methodology and theoretical background of the numerical methods used in this thesis. The literature study is presented in the introduction and in the theory behind numerical methods. Chapter 3 focuses on the numerical models and simulation set-up. The results are presented in Chapter 0 along with discussions. Conclusions are presented in Chapter 0. Chapter 6 discusses the future work based on the limitations defined at the beginning of the thesis. The references are listed in Chapter 7. Chapter 0 includes the appendix that holds all the additional information.

2 Methodology

This chapter presents the methodology used in the thesis for investigating interaction effects of wave parks. The numerical methods followed in the thesis are divided into 5 categories:

1. Numerical analysis of a single WEC system by parametric sensitivity analysis
2. Numerical modelling of WEC array
3. Hydrodynamic analysis
4. Structural response analysis
5. Power and interaction analysis

The numerical analysis in (1) aims to establish a reference WEC system with desired hydrodynamic and structural responses for various environmental conditions listed in Table 3-4. The WEC system has three subcomponents, a WEC buoy, mooring lines, and a PTO system. The WEC buoy responds to the wave forces through fluid-structure interaction and influence the motion of subcomponents through structure-structure interaction. Conversely, the mooring forces and motion also influence the dynamics of the WEC system. Therefore, the hydrodynamic analysis (3) and structural response analysis (4) are coupled and simulated together in time domain. The reference model analysed in (1) can then be used in the numerical modelling of the WEC array (2). The heave response from coupled time domain analysis of (3) and (4) can then be processed for power analysis. Through comparison and normalization with respect to the reference cases, the wave interaction effects are observed.

The study is divided into three phases - modelling, analysis, and post processing. In the first phase, the adopted single WEC model is used to model the wave park array in HydroD (DNV GL, 2017) and SIMA (DNV GL, 2022). Second, the coupled hydrodynamic and structural analysis is carried out in DNV GL SESAM package (DNV GL, 2019c) for various design parameters and environmental parameters described in Section 3. Finally, the post-processing of results from the analysis is discussed in detail. Parametric sensitivity study is performed throughout the project from modelling to the post-processing. Figure 2-1 illustrates the methodology followed in this thesis.

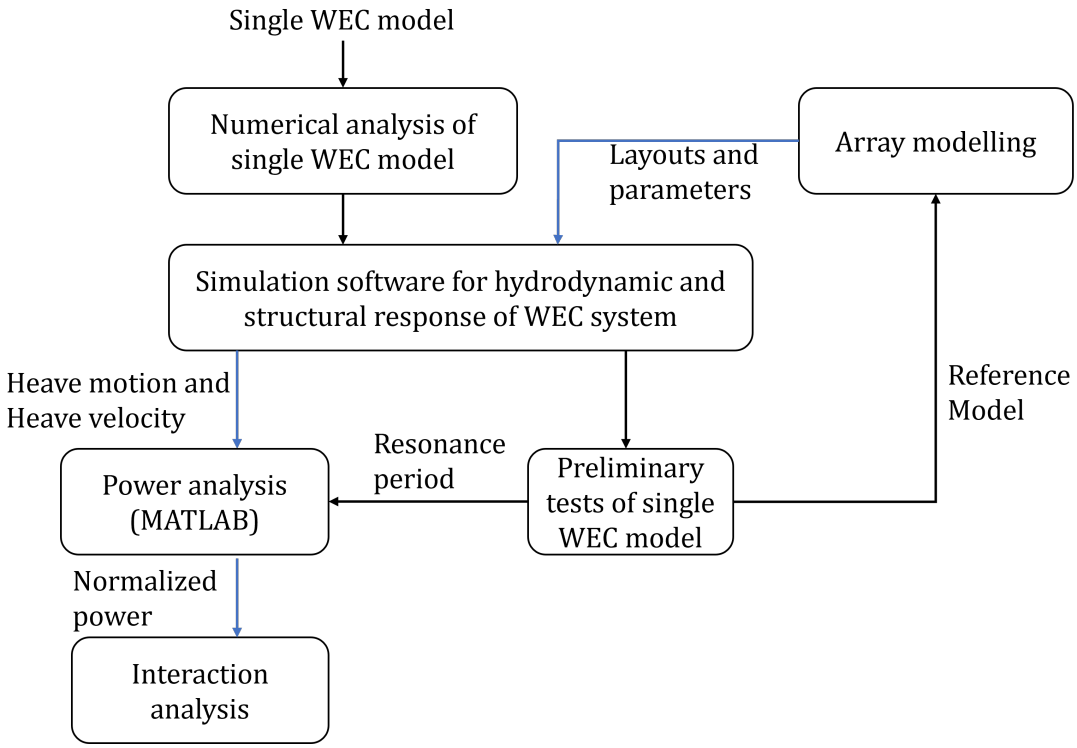

Figure 2-1 Illustration of the methodology for evaluating the interaction effects for different wave parks.

2.1 Hydrodynamic and structural response analysis

This study uses the coupled simulation method recommended by Yang et al. (2016). The numerical method captures various interaction effects in the complex WEC system. The multiple responses originating in the WEC system are classified as hydrodynamic response and structural response. The hydrodynamic response originates from fluid-structure interaction and the structural response from structure-structure interaction. The WEC motions due to wave forces transfers to its mooring components inducing an additional structural response, and vice versa. The frequency-domain simulations cannot capture the non-linearity of the mooring responses. Therefore, a coupled time-domain simulation method is utilized for the simulations.

The frequency-domain simulations are conducted in HydroD software (DNV GL, 2017) of the DNV SESAM software package (DNV GL, 2019d). The core solver in this software, WADAM (DNV GL, 2019d), uses the panel model of the CorPower WEC buoy and potential flow theory to compute several information of the WEC system, such as hydrostatic data, global responses of the WEC buoy, and coupled added mass terms for the hydrodynamic interactions in radiation and diffraction.

The time-domain simulations are conducted in the SIMA software (DNV GL, 2022) of the DNV SESAM software package. SIMA uses the results from the frequency-domain simulations and couples them with the point model of the WEC system. The core solvers utilized in this software, SIMO (DNV GL, 2019c) uses the point model of the WEC and RIFLEX (DNV GL, 2019a) uses the finite element model of the mooring to calculate the global WEC response of the WEC system in time-domain under various environmental loads.

Furthermore, Airy wave theory is used for the computation of environmental loads. This environmental load model is utilized by SIMA and HydroD for all the simulation conditions. The Airy wave theory is suitable for linear waves and this thesis focuses on the sea states with small wave heights using the Joint North Sea Wave Project (JONSWAP) spectrum, with a peak enhancement factor γ of 1.7 which is representative of most ocean regions; see Section 3.3.2. Table 2-1 shows the sub-models and their use in the corresponding core solvers used in simulations.

Table 2-1 : The sub-models corresponding to usage in core solvers used in coupled hydrodynamic-structural simulations.

Sub model	Usage	Theory	Core Solver
Environmental load model	External environmental loads acting on the WEC system	Airy wave theory	WADAM in HydroD SIMO and RIFLEX in SIMA
Panel model of the WEC Buoy	Hydrodynamic response of WEC buoy in frequency-domain simulation	First and second order three-dimensional potential theory	WADAM in HydroD
Point model of the WEC buoy	Motion and force response of the WEC buoy in time-domain simulation	Rigid body motion	SIMO in SIMA
Finite element model of mooring	Motion and force response of the mooring	Continuum mechanics theory for structural response	RIFLEX coupled with SIMO in SIMA

2.2 Power absorption analysis

The CorPower WEC model gives the heave motion of the buoy that can be converted to electricity. Based on the observed heave data from simulations, the power output can be calculated as instantaneous power output *P(t)*. The equation for power calculation is as shown in equation (2-1).

$$\boldsymbol{P(t) = C_{PTO} z^2_{rel(t)}} \tag{2-1}$$

where, z_{rel} is the relative velocity between the WEC buoy and the PTO system in the body fixed co-ordinates and C_{PTO} is the damping coefficient. The heave motion is calculated for different sea states. The damping coefficient C_{PTO} is the sum of useful damping (R_u) and linear loss damping (R_{loss}). The linear loss damping accounts for the machinery losses that is approximated to 25 kNs/m and kept linear for simplicity of the PTO model, the damping coefficient is shown in equation (2-2).

$$\boldsymbol{C_{PTO} = R_u + R_{loss}} \tag{2-2}$$

The damping coefficient is a measure of the WEC buoy to resist the motion caused by the environmental loads. The value of useful damping, denoted as R_u, is a varying parameter. It is assigned specific values depending on various sea states. The simulation run list in Section 3.3 provides a list of the useful damping values associated with different sea states used in this thesis. The overall power absorption, calculated across the entire simulation period and considering the number of WECs, is expressed through averaged power, and it is represented as:

$$\boldsymbol{P_a = \sum_{1}^{n=16} \frac{\left(R_u * \dot{z}_{rel}^2\right)}{Time\ Steps}} \tag{2-3}$$

Further, the heave data from the simulations is post-processed to interpret the WEC responses in terms of power produced. SIMA generates the WEC response in heave, and heave velocity along with multiple responses for the WEC system. The post processing tools in SIMA filters the required outputs and stores it in a database for further calculations. The postprocessing tasks were continually optimized both in SIMA and MATLAB (Mathworks, 2021) for calculations and result interpretation thought the study. MATLAB was used in the latter half of the post processing steps to perform calculations for the WEC response database generated by SIMA.

3 Numerical simulations

This chapter presents the numerical WEC model used in coupled simulations, see Section 3.1. The array configurations studied are presented in Section 3.2 and Section 3.3 presents the simulation run list.

3.1 WEC system description

The WEC model studied in the thesis is a heaving point absorber, shown in Figure 3-1. It consists of 3 main components: the PTO system, the mooring line and the WEC buoy. The floating WEC buoy is the main body of the WEC. This buoy produces hydrodynamic response through fluid-structure interaction with the environmental loads. The WEC buoy has additional drag elements to simulate viscous drag force of the body in heave, surge, and sway motions. In the scope of this study, the responses are filtered and only the heave response is considered for the power analysis.

The design of the WEC has a major impact on effects of the structural response. One of the major visible changes in design of the CorPower WEC's compared to other WECs is the single mooring element that extends down to the seabed. While some of the common concepts include mooring ropes and intermediate buoys, the stiff long mooring exhibits different structural response. While the moorings' main function is to hold the position of the buoy, differences in designs affect other aspects of the structural response.

The mooring line connects the floating buoy with a stationary anchor fixed to the seabed. The node at the seabed is free to rotate but is restricted in translation DOF to allow surge and sway motions of the WEC buoy. The mooring line is modelled as stiff rod that has very high torsional and bending stiffness.

The last component is the PTO System. Several features of SIMA offer flexibility in modelling. Using these features the behaviour of physical system with wave spring is replicated in the model. A negative stiffness is introduced as a coupling force between the WEC buoy and the anchor body (see Section 3.1.1). The water surface acts as the mean position ensuring the amplification of the WEC response to wave forces. Another coupling between the WEC buoy and the anchor body acts as end-stop. The end-stop limits the WECs overall motion, at +3.5 m and -3.5 m along the local *z*-coordinate of the WEC. These limits facilitate a combined displacement of up to 7 m. Additionally, a third coupling called pretension force between the WEC buoy and anchor body is introduced to ensure the buoy floats at its geometric centre in *xz*-plane. These couplings are further explained in the section below.

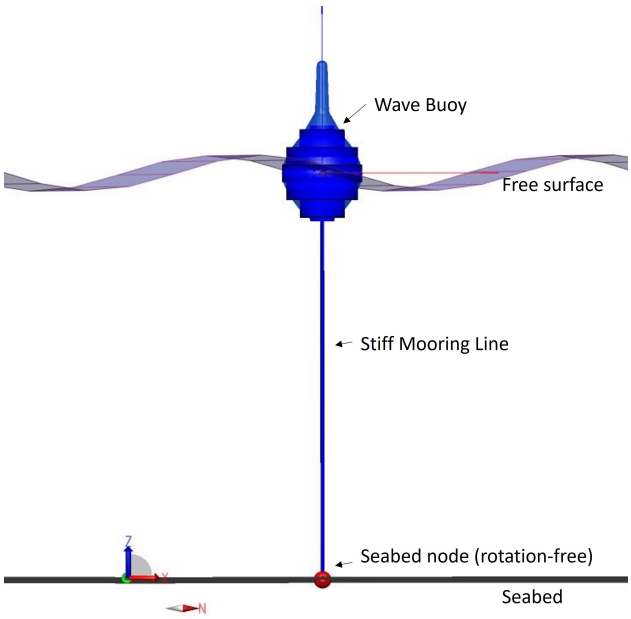

Figure 3-1: Single WEC model.

The model comprises 6 drag elements namely D1, D2, D3, ……D6 to compensate for the viscous forces. They are of different sizes and are designed along the buoy with constant heave and surge drag coefficients 0.25 and 0.50 respectively. Table 3-1 lists some of the important properties of the WEC buoy.

Table 3-1: Properties of WEC buoy.

Structural mass [kg]	60000
Mass moment of inertia Ixx and Iyy [kgm^2]	2.5e+06
Mass moment of inertia Izz [kgm^2]	5e+05
COG (x,y,z) [m]	(0, 0, 0.3145)

3.1.1 The negative stiffness

The negative stiffness is a distinguishing feature that is specific to the CorPower WEC system. The negative stiffness between the anchor and the buoy help amplifying the response nearly 3 times as indicated in the company's website for the tuned condition in favourable sea state (CorPower Ocean, 2023); see Section 4.1.3. A negative stiffness of -510 kN/m is used to amplify the buoy's motion. This stiffness becomes zero as the heave amplitude exceeds ±3.5 m. This whole mechanism is part of the PTO system. Figure 3-2 shows the negative stiffness used in the WEC model and Table 3-2 shows the magnitude of force that is required to obtain this WEC behaviour.

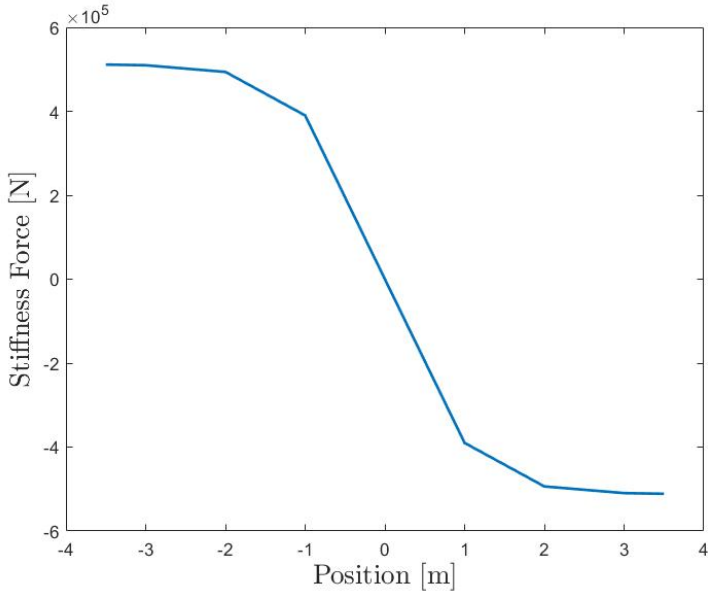

Figure 3-2: Negative stiffness.

Table 3-2: Stiffness force and position.

Position [m]	Stiffness force [N]
-3.5	5.11E+05
-3	5.10E+05
-2	4.94E+05
-1	3.90E+05
0	0
1	-3.90E+05
2	-4.94E+05
3	-5.10E+05
3.5	-5.11E+05

3.1.2 The pretension force

The pretension force is applied as a coupling between the anchor body in the seabed and the WEC buoy at free surface. The WEC buoy has a structural mass of 60 tonnes (see Table 3-1). The displacement required for the buoy to float in its geometric centre in the *xz*-plane is approximately 210 tonnes. Therefore, an additional 150 tonnes of weight need to be added to increase the draft of the buoy. This is done by applying a positive tensile force that holds these two bodies in constant tension. The magnitude of the force calculated is 1.49 MN. In other words, this force represents the additional buoyancy force that is generated when the WEC buoy floats in its geometric centre.

In the simulation model with 46 m water depth, the pretension force is kept constant for the variation from 46 m to 50 m accounting for waves and maximum heave motion of ±3.5 m. This ensures that the WEC buoy maintains the mean floating position when oscillating with encountered waves.

Similarly, for the simulation model with 55 m water depth, the pretension force is of the same magnitude as it depends on buoyancy and displacement. This force is applied as a constant over the range of 55 m to 59 m accounting for maximum heave motion of ±3.5 m.

3.1.3 The end stop

To prevent damage to the PTO system and the WEC buoy, limits are imposed on the vertical motion of the PTO device. These limits are enforced using end dampers, which apply an end stop force represented by the end stop curve, as shown in Figure 3-3.

The equation of the end stop curve is given by:

$$F_{es}(x) = -c\frac{x}{|x|}\,(|x| - x_{es})^n * u\,(|x| - x_{es}) \tag{3-1}$$

where:
- x_{es} is the end stop position,
- x is the current position,
- the constants c and n can be adjusted to obtain desired results, and
- u is the heave-side step function.

The parameter n alters the degree of the equation, increasing or decreasing the stiffness force accordingly. The WEC model is developed to replicate the actual mechanism of CorPower's WEC system. The end stop curve used in this thesis has following parameters listed in Table 3-3.

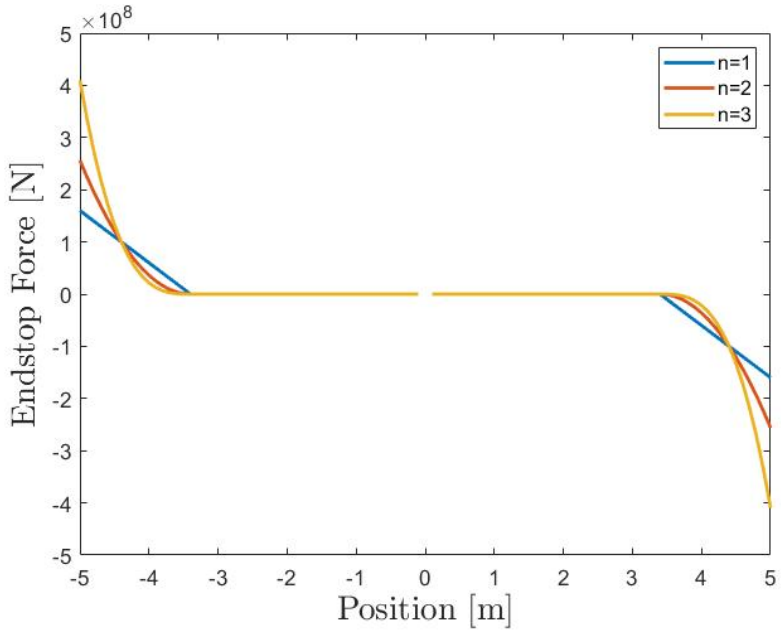

Figure 3-3: Endstop force curve.

Table 3-3: End stop parameters.

Parameters	Values
X_{es}	3.4
n	2
c	$1x10^8$ N/m^2

3.2 Array modelling

Two arrays of wave parks were considered, and they were together with CorPower identified as wave parks of interest. Several studies, have shown that linear array configuration performs better than other closed array types (Sinha et al., 2016) and (Engström et al., 2013). This performance advantage is observed when the wave direction is normal to the array, an important consideration in the array installation process.

Figure 3-4 shows the two array configurations studied in this thesis. The arrays consist of 16 single WEC units arranged in two different configurations, the first array configuration studied is a square grid with each unit separated by the same distance apart from the other nearest WEC in the horizontal plane. The array consists of 4 rows and 4 columns, represented with 4x4 WEC array shown in Figure 3-4: WEC array: (a) 4x4 layout, WEC array layout 8x2 (b)Figure 3-4a. The second array configuration of 16 WECs is set up as 2 rows by 8 columns i.e. a 8x2 WEC array. The 8x2 array is oriented such that the incident wave hits all 8 WECs of the row at the same time.

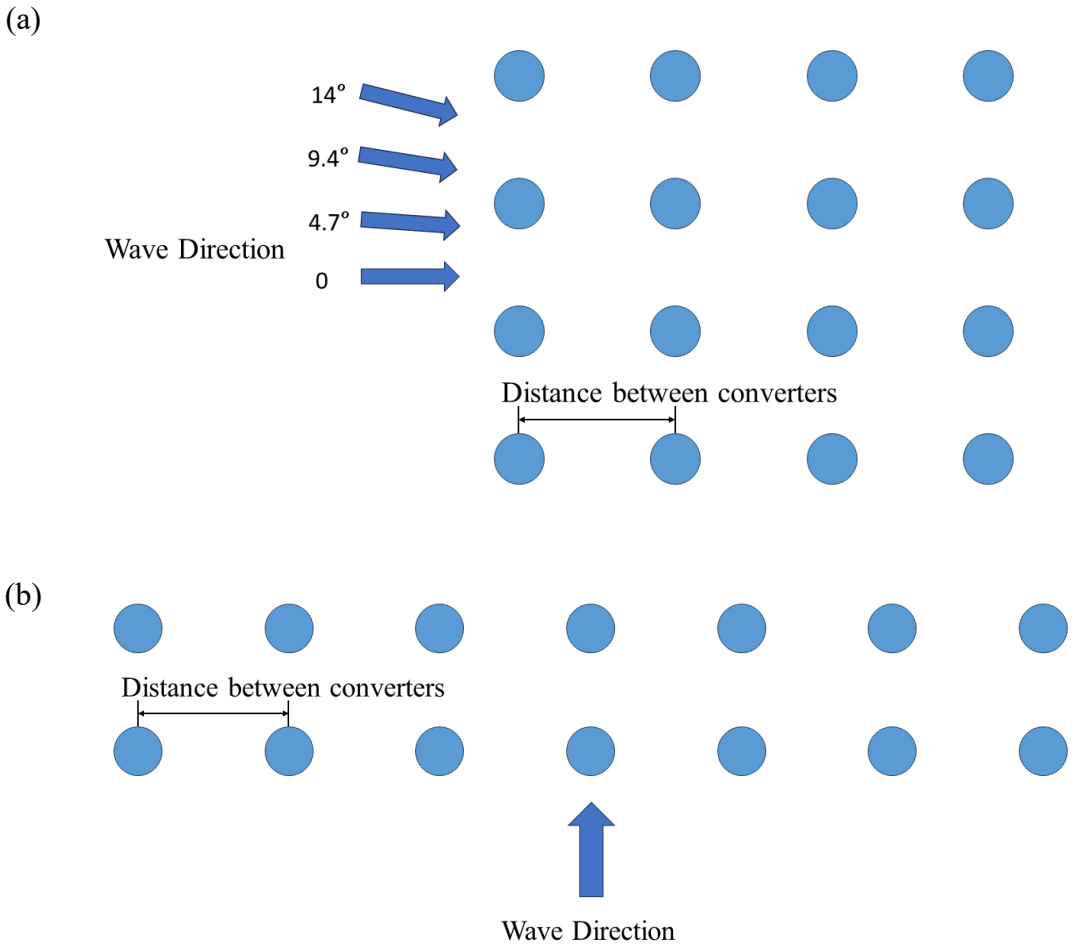

Figure 3-4: WEC array: (a) 4x4 layout, WEC array layout 8x2 (b).

Figure 3-5 shows the three separation distance parameters of 50, 150 and 200 m considered in this thesis. The aim is to study the array performance with these separation distances and their impact on the hydrodynamic interaction between the WECs. The short distance between WECs experiences stronger interactions. Conversely, the larger distance reduces the interaction effects between wave energy converters. Larger distances can also provide more space for mooring and maintenance

activities at the cost of more area used per kW generated. Medium distance of 150 m was considered based on the CorPower WEC array CorPack.

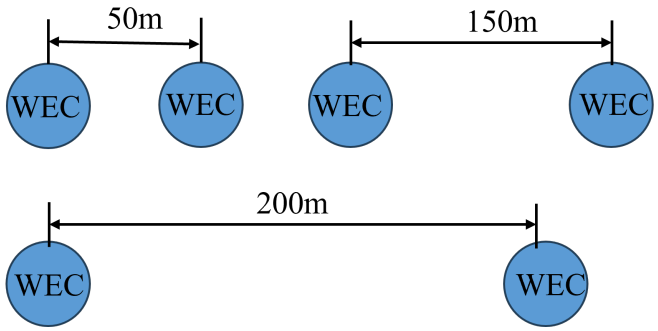

Figure 3-5: WEC distance parameter.

3.3 Simulation run list

A simulation run list presented in Table 3-4 was composed with guidance from CorPower. One purpose of the simulated conditions was to evaluate the impact of environmental parameters over the power production of WEC array. The environmental conditions, referred to as sea states from here on, are broadly classified into regular sea states and irregular sea states. An additional distance parameter 'D' was included and was varied as 50, 150 and 200 m.

Table 3-4: Simulation run list.

	S.no	Sea states	Wave height [m]	Wave Period [s]	Damping [KNs/m]	Direction
Regular Low	1	RL1	1	5	137	0º
	2	RL2	1	6	115	0º
	3	RL3	1	7	94	0º
	4	RL4	1	8	80	0º
	5	RL5	1	9	78	0º
	6	RL6	1	10	88	0º
	7	RL7	1	11	107	0º
	8	RL8	1	12	129	0º
	9	RL9	1	13	152	0º
	10	RL10	1	14	176	0º
	11	RL11	1	15	199	0º
Regular High	12	RH1	4	5	144	0º
	13	RH2	4	6	124	0º
	14	RH3	4	7	107	0º
	15	RH4	4	8	163	0º
	16	RH5	4	9	227	0º
	17	RH6	4	10	287	0º
	18	RH7	4	11	343	0º
	19	RH8	4	12	395	0º
	20	RH9	4	13	445	0º
	21	RH10	4	14	494	0º
	22	RH11	4	15	541	0º

Irregular Low	23	IRL1	1.75	7.5	90	0º
	24	IRL2	1.75	9.5	86	0º
	25	IRL3	1.75	11.5	118	0º
Irregular Medium	26	IRM1	2.75	7.5	95	0º
	27	IRM2	2.75	9.5	152	0º
	28	IRM3	2.75	11.5	226	0º
Irregular High	29	IRH1	3.75	7.5	115	0º
	30	IRH2	3.75	9.5	237	0º
	31	IRH3	3.75	11.5	341	0º
Irregular Low Water depth 55m	32	IRLW1	1.75	7.5	90	0º
	33	IRLW2	1.75	9.5	86	0º
	34	IRLW3	1.75	11.5	118	0º
Irregular Low Layout 8x2	35	IRLL1	1.75	7.5	90	0º
	36	IRLL2	1.75	9.5	86	0º
	37	IRLL3	1.75	11.5	118	0º
Irregular Low Angle	38	IRLA1	1.75	7.5	90	4.7º
	39	IRLA2	1.75	9.5	86	9.4º
	40	IRLA3	1.75	11.5	118	14º
Irregular High Water depth 55m	41	IRHW1	3.75	7.5	115	0º
	42	IRHW2	3.75	9.5	237	0º
	43	IRHW3	3.75	11.5	341	0º
Irregular High Layout 8x2	44	IRHL1	3.75	7.5	115	0º
	45	IRHL2	3.75	9.5	237	0º
	46	IRHL3	3.75	11.5	341	0º
Irregular High Angle	47	IRHA1	3.75	7.5	115	4.7º
	48	IRHA2	3.75	9.5	237	9.4º
	49	IRHA3	3.75	11.5	341	14º

3.3.1 Regular waves

The regular waves are sinusoidal unidirectional waves with a single wave height and wave period. In this thesis, the regular waves are further divided into low waves of 1 m wave height and high waves of 4 m wave height each of these having wave period range from 5 s to 15 s with 1 second time interval.

This set of regular waves are an important part of the study as they provide the hydrodynamic response of WEC that is directly dependent on the single set of wave period and wave amplitude. The data obtained from the basic responses from single/regular waves provide a foundation for the responses observed on complex environmental conditions.

3.3.2 Irregular waves

The irregular waves are short-crested multidirectional waves. These waves are representative of the actual sea conditions, i.e., natural waves. They are a composition of many sine waves with different heading angles. In theory, the irregular waves can be decomposed into individual waves with different frequencies using Fourier transforms.

Because of the random nature of these natural waves, they are always defined by a statistical distribution. In this thesis, the JONSWAP spectrum in the wave frequency domain was used with a peak enhancement factor γ = 1.7. The JONSWAP spectrum (Joint North Sea Wave Project) defines the distribution of energy with frequency within the ocean. It is a fetch-limited version of Pierson-Moskowitz (PM) spectrum. The value of γ ranges between 1 to 7, and at 1, the JONSWAP and the Pierson-Moskowitz (PM) spectra are the same; default γ value for the North Sea is 3.3 and lower values such as 1.7 that is used in this thesis is more representative of most ocean regions.

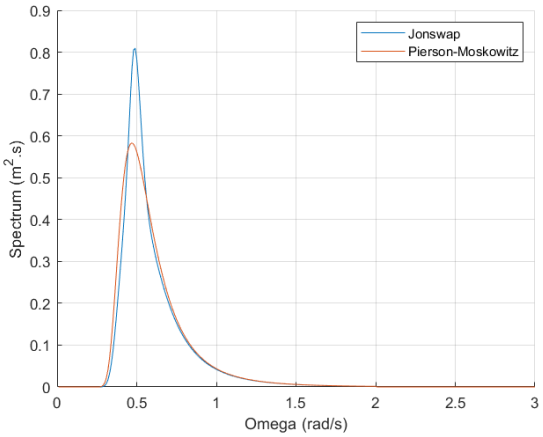

Figure 3-6: JONSWAP Spectrum γ = 1.7.

In SIMA, the sea states are developed from the moment of application. In the initial stages of the simulation, a simple comparative study was made between different simulation lengths of one-third of an hour, an hour, and 3 hours of irregular sea states to observe the maximum significant wave height in these conditions. Due to the sheer number of simulations and the computational time associated with it, the simulation length of these sea states is reduced to 1000 s.

The irregular waves are further grouped into low, medium and high waves with 1.75 m, 2.75 m and 3.75 m as the significant wave height (H_s). The significant wave height is the mean of the highest third of waves also denoted by $H_{1/3}$. Each of these waves in sea states are combined with three peak wave periods (wave periods of highest energy) of 7.5 s, 9.5 s and 11.5 s to define the sea states.

3.3.3 Bathymetry

Variable bathymetry is not considered in this study; the seabed for this study is constant for the whole simulation area. The water depth selected for this study has significantly less impact on the wave properties. The impact of water depth is studied by considering two values 46 m and 55 m depth. The mean floating position of the WEC system is changed from 46 m to 55 m. The couplings, such as negative stiffness, pretension force and end stops, are modified to operate in the 55 m water depth. The pretension force remains the same with a modified mean position since it depends on the buoyancy and weight of the WEC buoy (see Section 3.1.2). The changes in depth and their impact are further discussed in the results Section 4.1.3 and Section 4.2.2.1.

The environment setup does not consider currents or wind forces. The responses obtained for the analysis are entirely based on the sea states input to the simulation. The structural responses are obtained from wave forces in regular and irregular seas.

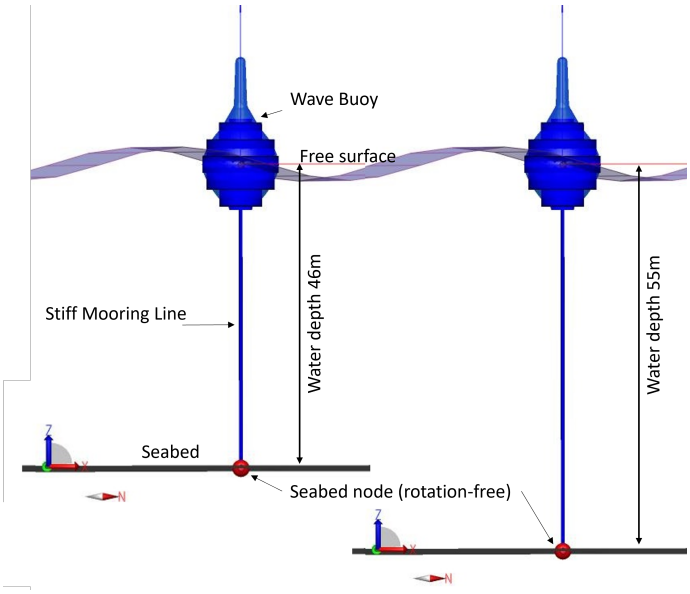

Figure 3-7: WEC system with two water depth parameters with the same coupling forces.

4 Results

The chapter presents the results from numerical simulation and a discussion of these. The results are divided into three parts: Section 4.1 presents the initial tests conducted on the WEC system, the results of power absorption analysis for the selected simulations are presented in Section 4.2, followed by interaction analysis results in Section 4.3 for the selected simulations together with parametric sensitivity study for these results.

4.1 Initial tests and comparison

The power absorption analysis as the name suggests is performed by interpreting the buoy response that is in the form for heave and surge/sway, in terms of power produced by the WEC system. The calculations are described in Section 2.2.

4.1.1 Free decay test

The simulation matrix presented in Section 3.3 has most of the environmental conditions near the resonance period of the WEC system, especially for the irregular sea states. Therefore, it is important to analyse the resonance frequencies of the WEC system for different parameters. The only physical parameter that changes the design values of the individual WEC system is the water depth parameter, the effects of which are further explained in Section 4.1.2

The free decay test is conducted numerically to determine the resonance periods of the WEC model. To perform these tests, the model is subjected to an external force for a certain time until it reaches a steady state, and the force is removed. As a result, the WEC system tends to retain its equilibrium position from the externally excited position. While the buoy oscillates resembling a damped waveform, the mean of these wave periods will give the resonance period of the WEC system. Four simulations were performed to determine the resonance time periods, two for 46 m water depth and two for 55m water depth among these two, one simulation gives the heave motion, and the other simulation gives surge/sway of the WEC System. Both tests were performed in an environment with a very high wave period and low wave amplitude, the effects of which are negligible on the responses of the WEC.

Figure 4-1 shows the free decay of the heave motion. A force of 30 kN is applied in the positive *z* direction of the buoy's COG and then released after 300 s. The wave buoy then oscillates back to its mean (equilibrium) position. The damped waveform is analysed, and the peaks of this wave form are measured. The difference between these peaks gives the heave resonance period of 7.5 s. This value is representative of the real physical model.

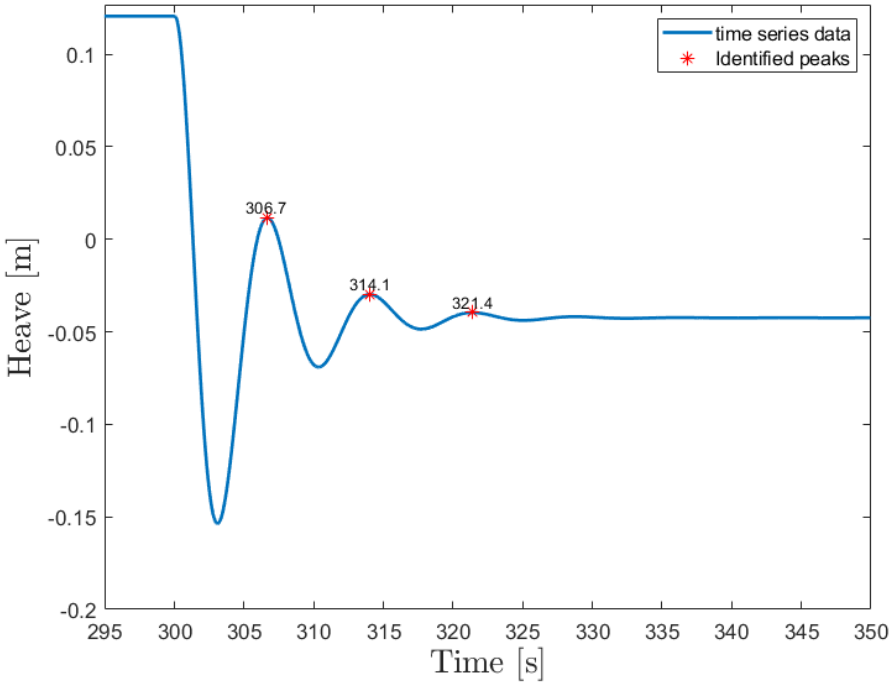

Figure 4-1: Free decay for heave resonance.

Figure 4-2 shows the free decay of the surge motion. While the heave test was performed in the *z*–coordinate axis of the buoy, the surge test was performed in the *x*-coordinate axis. The damped waveform of the WEC system that oscillates back to its mean position is recorded, and the difference between the peaks of this waveform gives the resonance time period. The surge resonance period is calculated to be 15.3 s for 46 m water depth and 16.8 s for 55 m water depth.

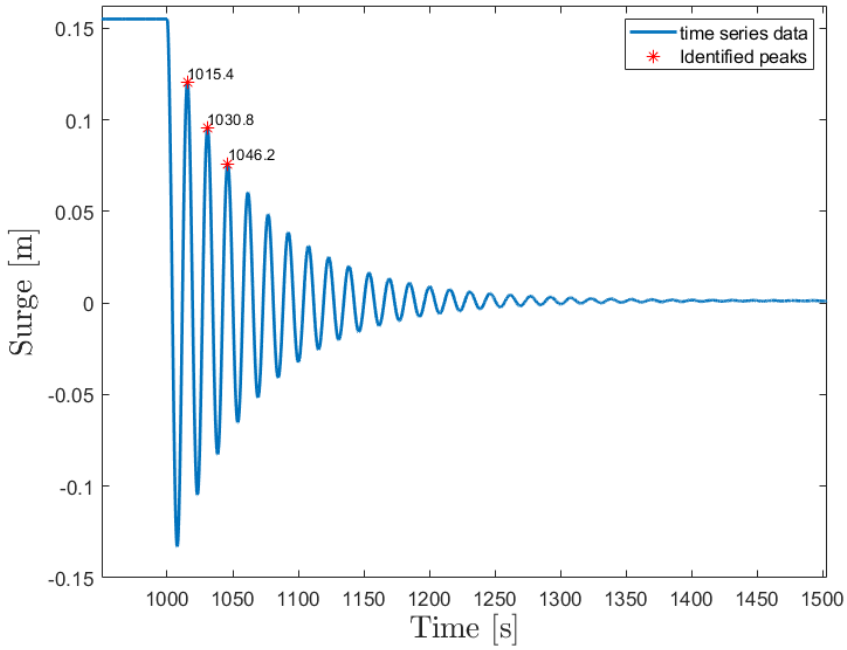

Figure 4-2: Free decay for surge resonance.

Table 4-1: Resonance periods of the WEC system.

Water depth [m]	Heave resonance period [s]	Surge resonance period [s]
46	7.5	15.3
55	7.5	16.8

As shown in Table 4-1 a difference of 1.5 s is seen in the surge resonance of the WEC system. This plays a major role in the depth influence study described further in Section 4.1.3.1. The resonance periods obtained are within the range of the resonance periods of the physical system used by CorPower. The system has a heave resonance range of 7.5 s to 8.5 s, and the surge resonance range is 15 s to 17 s. Hence, the model is verified.

4.1.2 Reference condition without interaction effects

A single unit WEC could have been used as a reference WEC, but an array of 4x4 layout was used where interaction effects were disabled in the simulations. The results from fully coupled simulations were then compared to these base models, which helped to analyse the results (i) for the entire wave park and (ii) for the individual WECs in the same locations.

4.1.3 WEC response in regular sea state

The regular waves were the first set of simulations. The unidirectional wave environment was set up in SIMA, and the simulations were conducted according to the order described in Table 3-4. Although the regular waves are only theoretical and do not represent the sea state in the real world, it is an important part of the study. The simulation results provide a detailed WEC response in a simple waveform in each set of wave amplitude and wave periods. The resonance period of the WEC plays an important part in this study.

The WEC response for regular sea state RL1 – RL3 (i.e., wave amplitude 0.5 m and wave periods ranging from 5 s to 7 s) at 46 m water depth and pretension force of 1.49 MN is presented in Figure 4-3. Here it is observed that the system is performing as expected in near the resonance periods. It is designed in a way that the response of the WEC buoy is nearly three times the wave amplitude to replicate the physical WEC model of CorPower.

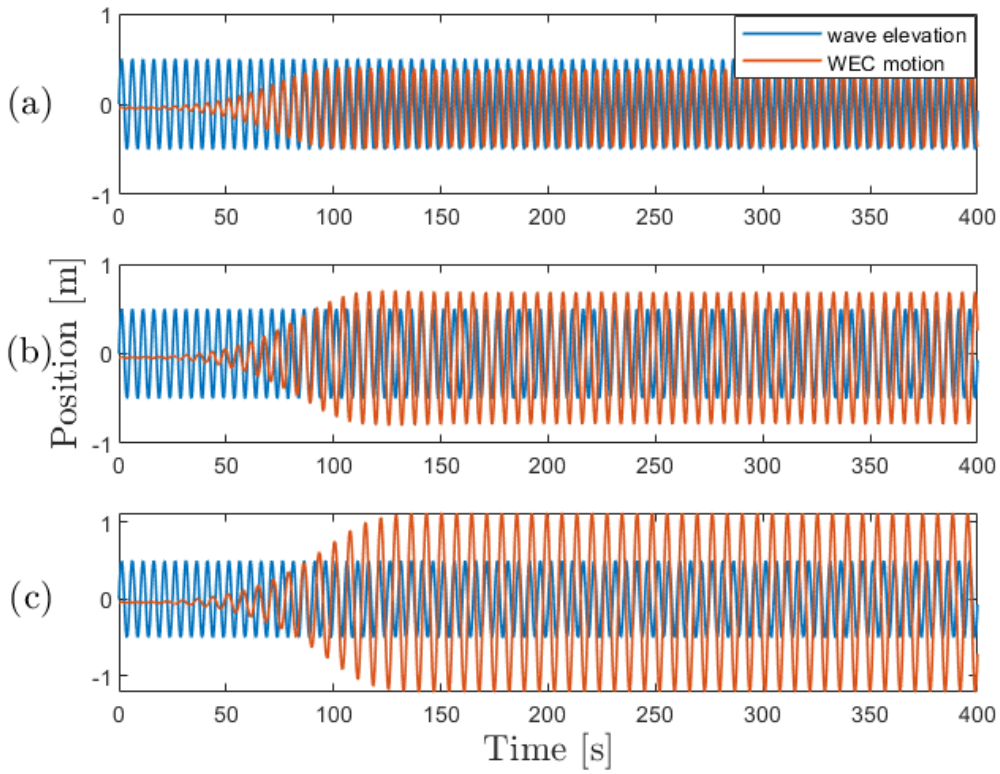

Figure 4-3: WEC system subjected to regular waves with wave amplitude of 0.5 m and wave periods of (a) Tp = 5 s, (b) Tp = 6 s (c) and Tp = 7 s.

While the power absorption analysis depends mainly on the heave motion of the WEC, the surge/sway motions sometimes hinder the heave motion. The energy absorbed by the WEC during this combined response is then split up into multiple responses of heave and surge. Only a limited amount of energy could be absorbed from the waves. As per the energy conservation law, if the surge response is amplified, the energy absorbed to produce a heave response is lesser, resulting in lower power production. This phenomenon is further explained in Section 4.1.5

4.1.4 WEC response in irregular sea state

The irregular sea states defined in the simulation matrix in Section 3.3 are the main environmental parameters considered for this study. The water depth for all the simulations was 46 m, except in the simulations that compare two different depths. The comparison between the WEC array responses in these sea states are further discussed in Section 4.2.2.

The individual WEC response is as shown in the Figure 4-4. In this case a sea state of significant wave height (H_s) of 1.75 m with the peak period (Tp) of 7.5 s is taken with 0^0 average wave propagation angle. In regular waves analysis it is observed that near resonance periods the WEC performs at its maximum power output. This is also evident in the figure below, where the motions of the WEC is maximised at larger wave heights together with heave resonance.

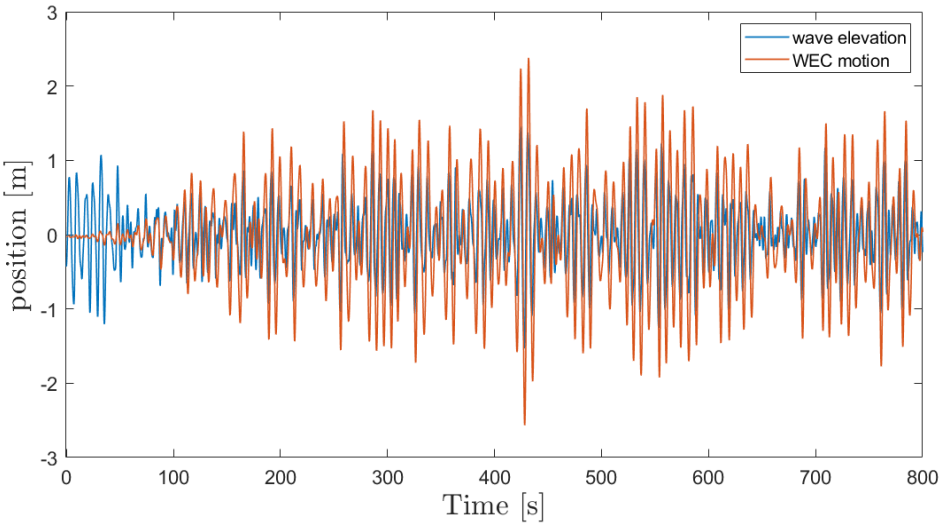

Figure 4-4: WEC response in irregular wave of Hs = 1.75 m and wave period = 7.5s.

4.1.5 WEC response at resonance period

Figure 4-5 shows the heave response of the WEC system in the RH5 sea state. It is observed that the response waveform is not full as compared with Figure 4-3c. The WEC behaves in a way that could be considered a repeating pattern. In the Figure 4-5, after the WEC has achieved a state of maximum excitation, it exhibits the waveform where each larger excited response is succeeded by a smaller response. This pattern repeats itself as long as the WEC is in resonance with the wave period. The resonance period for heave, however, is found to be 7.5 s (see Section 4.1.1).

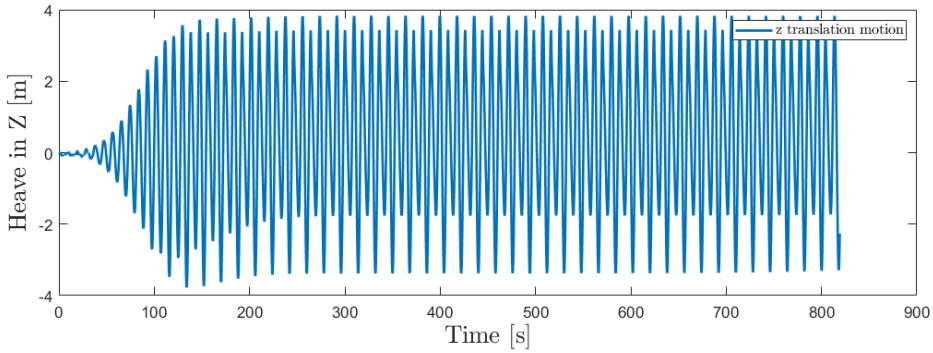

Figure 4-5: Heave response of WEC system at wave amplitude = 2 m and wave period = 9 s (RH5 sea state).

To analyse this behaviour further, the WEC response in the horizontal plane (water plane) was studied. It is found that near half the resonance period of surge/sway (see Table 4-1), the WEC motions increase to a very large number at about 12 m in the direction of the incident wave as seen in Figure 4-6a. The response in the *y*-direction (perpendicular to the incident wave) is small in comparison and is within the range of +/- 2 m from the origin until 700 s.

This WEC motions when combined, exhibits a pattern as shown in Figure 4-6 c in the horizontal water plane (*xy*) of the WEC. This figure is plotted for a small sway amplitude of +/-0.25 m, which lies in the time range of 200 s to 500 s in Figure 4-6b. From these figures It is evident that the surge/sway resonance plays an important role in either hindering or adding to the heave response of the WEC. This directly affects

the power output of the WEC. The effects are seen as early as the WEC tries to achieve a steady state at the 150 s mark in Figure 4-5.

(a)

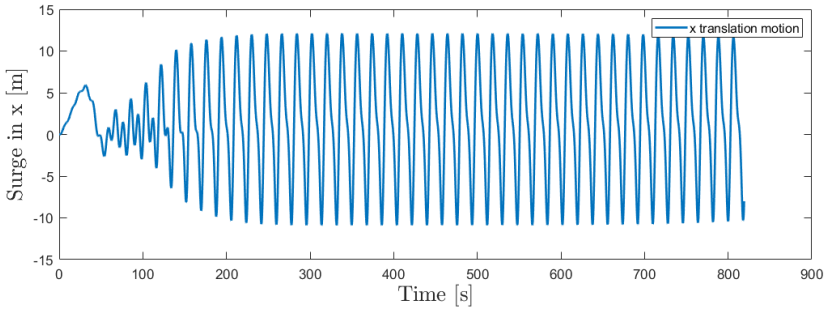

(b)

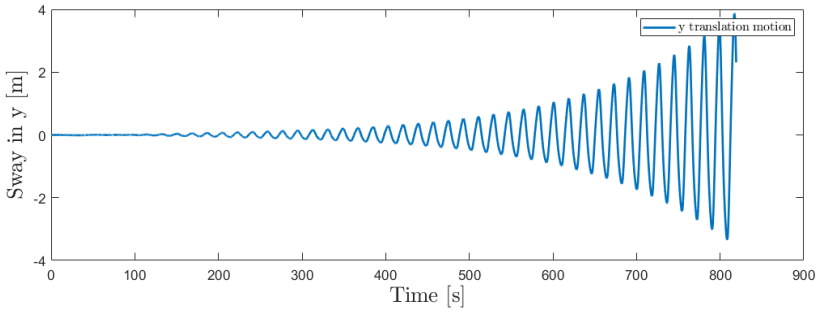

(c)

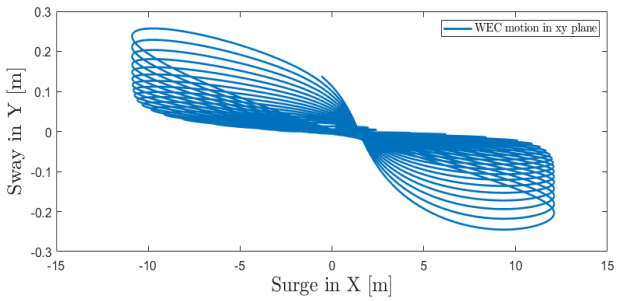

Figure 4-6: Surge/sway response of WEC system near resonance: x translational motion – surge (a), y translational motion – sway (b) and combined surge and sway in the horizontal plane of WEC (c).

4.2 Power analysis

This section presents the results from the power analysis as obtained from the heave response of the WEC array. The first subsection discusses about the power performance in the regular sea states, followed by irregular sea state in the second subsection and finally the comparison of the effects of different parameters in the irregular sea states.

4.2.1 Regular sea state

The regular waves are theoretical sine waves with a single amplitude, time period and direction. The power analysis of WEC array in these conditions provides the data necessary to understand the behaviour of WEC in a complex wave environment i.e., the irregular waves. In this first simulation set for regular waves, the wave amplitude is kept constant at 0.5 m and time period is varied from 5 s to 15 s. These make up to 11 sea states and an additional distance parameter is varied as 50 m, 150 m and 200 m.

4.2.1.1 Regular low

Figure 4-7 shows the power produced in the regular low seas and a comparison with the reference condition without interaction effects. As the wave amplitude is kept constant, the response of the WEC array is entirely dependent on the wave period and interaction effects of WECs downstream of the array. The power output shows a gradual increase in trend from RL1 to RL3 for all the array distances and reference condition. This behaviour is similar to the WEC response observed in the Figure 4-3. As the wave period nears the half resonance period of surge a dip is seen in the trend lines of power output. This observation is explained in detail in Section 4.1.5. as the time period increases, the power output trend regains its former projected path and gradually decreases and becomes stable at higher wave periods as it moves away from resonance.

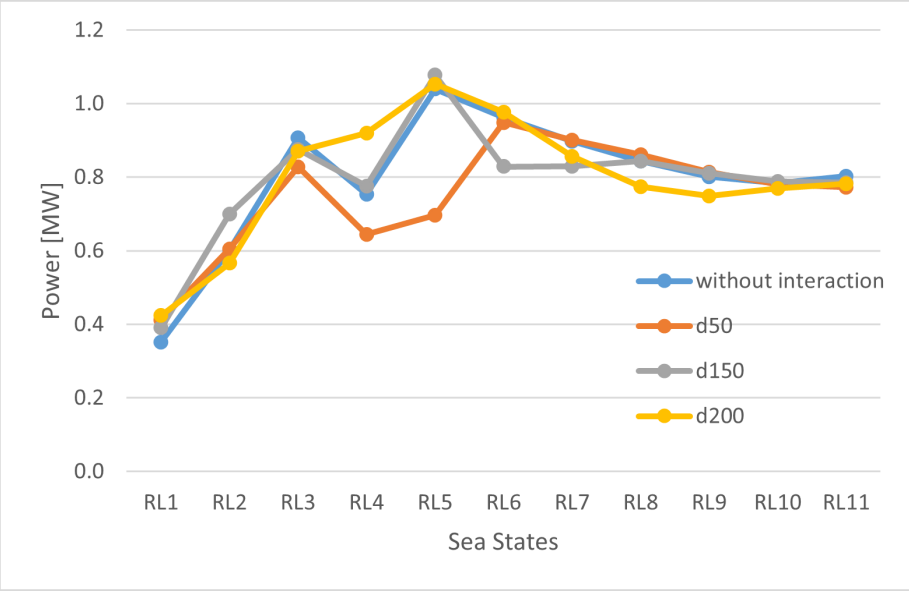

Figure 4-7: Power produced in regular low waves.

4.2.1.2 Regular high

In this section the regular high sea states are analysed, where the high seas have a constant wave amplitude of 2 m and wave period ranging from 5 s to 15 s, similar to that of regular low simulation set. Figure 4-8 shows the comparison between power output trend of the WEC in regular high seas and regular low seas for 150 m array distance.

The effects of both wave amplitude and wave period can be seen here, both parameters define the shape and magnitude of the power trend. The difference in magnitude of power output from RL sea states and RH sea states is directly dependent on the wave height the WEC is subjected to the slope, however, is dependent on the encountered wave period. As it is quite evident, the presence of a massive dip in the trend line of RH sea state is due to the combination of both wave amplitude and wave period increasing the surge motion observed in resonance. The power trend begins a downward slope at the wave period of 6 s, while it can be seen in Figure 4-7 that the power still increases until wave period 7 s. One of the reasons for this shift in the dip can be related to the wave amplitude. Since high amplitude produces a high response, this increases the surge/sway motion of the WEC observed in Figure 4-6c.

Another reason for this behaviour is that the surge/sway resonance period is calculated at a constant water depth with a fixed mooring length and little to no heave motion. It was seen that the mooring length significantly increases the surge resonance of the WEC system (see Section 4.1.1). When the WEC system is in a favourable sea state producing maximum heave response, a total vertical travel distance of 7 m is observed i.e., +/-3.5 m. In each of the heave response the mooring length constantly changes, and the surge resonance period cannot be considered a constant for this matter. Hence the downward slope of the power output can be related to how long the WEC system is out of the water in positive extension of the mooring. This results in more sway because of reduced buoyancy.

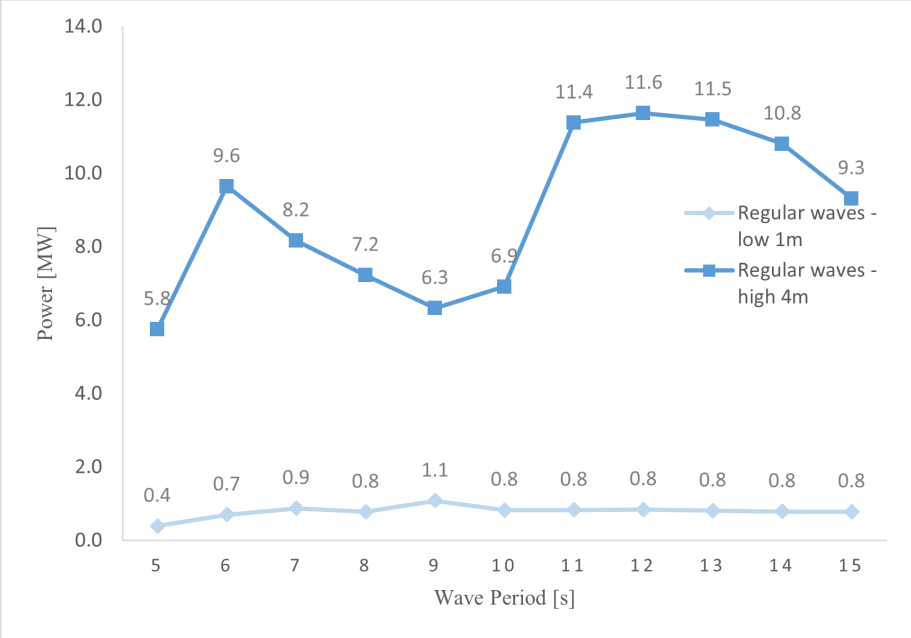

Figure 4-8: Comparison of power produced in regular high and low waves at 150 m WEC distance.

4.2.2 Irregular sea state

This thesis focuses mainly on interaction effects for realistic the real-world scenario. This means that all the simulations and comparison from this section onwards are a comparison of power and interaction effects with irregular waves as the environment. As in the case of establishing a baseline for comparison i.e., a case without interaction, it is also necessary to establish another baseline condition to proceed further in the analysis. The comparison of different parameters such as water depth, WEC array layout and the average wave propagation direction need a reference condition, and this is done by keeping the distance parameter as a constant at 150 m.

Another reason to make this simplification is that the CorPower Corpack WEC array has a distance of 150 m between its converters and hence it is of more importance to analyse this distance and make a comparison of different parameters. In the first set of simulations, only the significant wave height (*Hs*), peak wave period (*Tp*) and distance (d) parameters are varied and compared with the condition without interaction. The Figure 4-9 shows the power performance in 9 different sea states IRL1 to IRH3 that are a combination of significant wave height (Hs) ranging from 1.75 m to 3.75 m and peak wave period (*Tp*) ranging from 7.5 s to 11.5 s.

The trend observed in this analysis is a gradual positive slope. This is because the sea states are in the increasing order of *Hs* and *Tp*. The power is directly dependent on the wave height the buoy encounters since these simulations are in the range of resonance period for heave and surge. One major observation for these results is the interaction effects in most sea states are constructive and aid in maximising the heave response. It is also seen that the effects of resonance, i.e., the massive dip in power trend of regular waves as seen in Figure 4-7 are more suppressed. One reason for this is that the irregular waves are composed of many waves with different wave periods. The WEC fails to be stuck in a prolonged resonant state, although this resonance aids in increased heave response in that time instant. The buoy quickly recovers when it encounters other waves at different incident angles. There are few cases where the WEC buoy gets stuck in an excited position for a longer period than predicted.

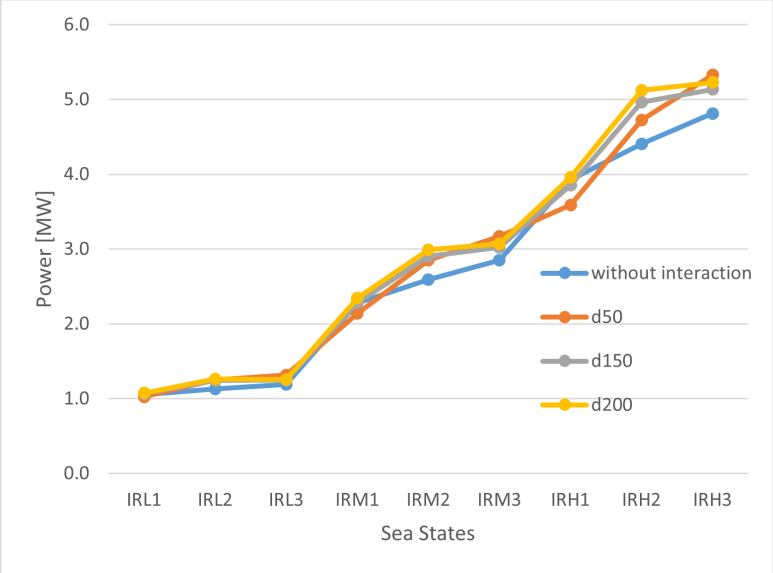

Figure 4-9: Power produced in irregular waves.

4.2.2.1 Water depth influence

The study focused on irregular sea states at two specific water depths: 46 m and 55 m. As the water depth increases, it impacts the length of the mooring line, leading to greater forces with negative stiffness.

Examining the Figure 4-10, it is observed that the rise in power between two water depth models is minimal, not exceeding 1%. The increase in water depth lacks significant impact in this regard, making it challenging to discern noticeable improvements in power performance.

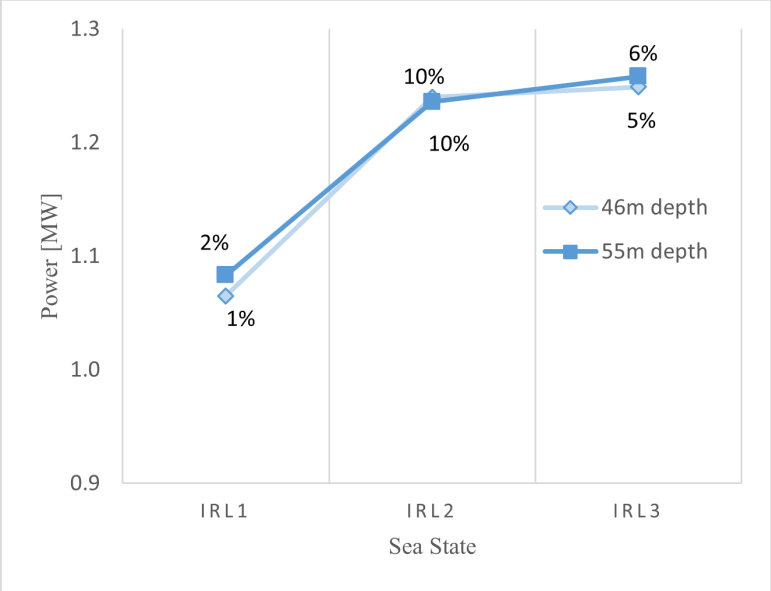

Figure 4-10: Influence of water depths for the 4x4 WEC array under irregular sea state IRL1-3.

4.2.2.2 Layout influence

This section studies the power performance of two array layouts (see Section 3.2). The Figure 4-11 illustrates how the layout impacts the power performance of the WEC array, particularly for the interaction effects across three IRL sea states.

The power performance of the 8x2 layout stands out in the sea state IRL1, while it significantly decreases in the sea states IRL2 and IRL3 compared to the layout 4x4. The reasons behind the changes in power performance are further explained in Section 4.3.2.2, which gives detailed information about how much power each WEC produces in both layout types.

For the 8x2 layout, the rows are facing the incoming waves and experiences relatively less interaction. This interaction impact becomes noticeable in the power output of the second row. However, in the 4x4 layout, the interaction effect becomes more pronounced, especially in the first row, which then contributes to decreased power output in the following rows, resulting in lower overall power production.

In the IRL2 and IRL3, the 4x4 layout benefits from favourable interaction effects. However, the 8x2 layout experiences destructive interaction in IRL3, resulting in a 4% lower interaction effects compared to cases without interaction. This discrepancy arises because interactions enhance the performance of WECs in the second and third rows of the 4x4 array. Conversely, in the 8x2 array, the performance of the first row is substantially reduced, as depicted in Figure 4-11 and Figure 4-18

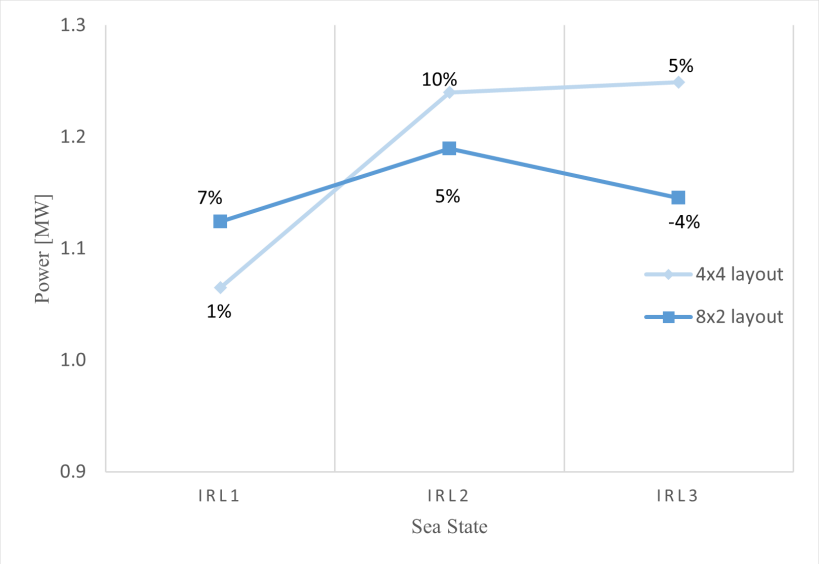

Figure 4-11: Influence of WEC array layouts 4x4 and 8x2 unde irregular sea state IRL1-3.

4.2.2.3 Wave encounter direction angle

This section studies the power performance with different wave encounter angle. The study is compared with the reference case with the 0-degree encounter angle. The interaction effects for the wave angle 9.4 degrees in the IRL2 is observed to be 5% higher compared to the case without interaction. While it is 4% more for angles 4.7 and 14 degrees for IRL1 and IRL3 sea states respectively. The interaction effects for the 0 degree are significantly more for IRL2 and IRL3 sea states. The encounter angle does influence the interaction effects as changing the angle determines the number of WECs that are affected by the interaction waves.

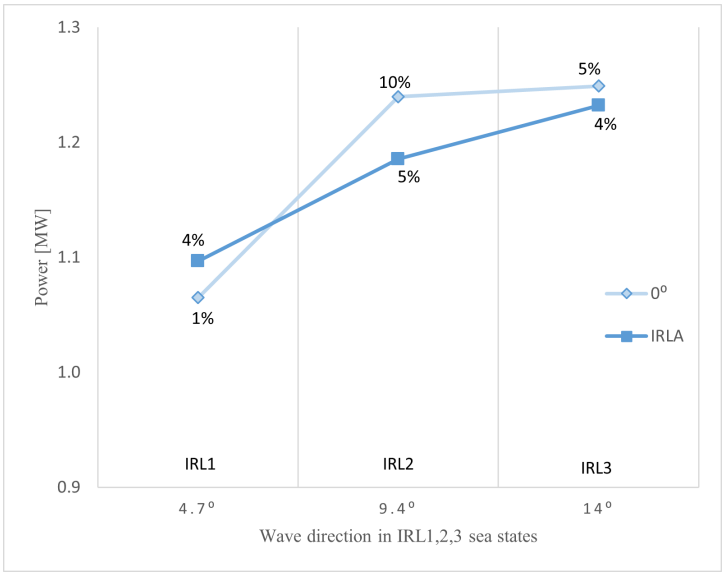

Figure 4-12: Power output of 4x4 wave park at different wave direction under irregular sea state IRL1-3.

4.3 Interaction analysis

This section presents simulation results for interaction effects in regular seas and irregular seas and a comparison with parameters such as water depth, WEC layout and incident wave angle. The interaction between the waves give rise to two types of interaction behaviour, constructive and destructive.

A simpler way to analyse these effects is by comparing how the array performs with how it could perform at its best. To do this, the performance for just one WEC system is calculated and then multiply that by the total number of WECs in the array. This helps create a reference condition to analyse the effects more clearly and understand how the waves interact in the array and it is referred to as interaction factor. As shown in Eq. 4-1:

$$Interaction\ factor, I_p = \frac{P_i - P_{ref}}{P_{ref}} \tag{4.1}$$

where, P_i is the power produced with interaction and P_{ref} is power produced without interaction effects.

4.3.1 Regular sea state

The results from the power analysis are further analysed to determine the interaction factor for these simulations. The power produced from the regular low seas are compared with the reference condition.

4.3.1.1 Regular low

To calculate the interaction factor, the reference WEC array is simulated through all environmental conditions and design parameters as depicted in the simulations run list in Section 3.3. The power output from these simulations is compared with outputs from corresponding simulations that include the interaction effects. The difference in power directly relates to the interaction factor.

Figure 4-13 shows the interaction factor for regular low sea state with wave amplitude of 0.5 m and wave period ranging from 5 s to 15 s, for WEC arrays set at various WEC distances apart. The positive interaction factor indicates constructive interaction, and the negative interaction factor indicates a destructive interaction. One distance performs better than the rest i.e., the 150 m distance.

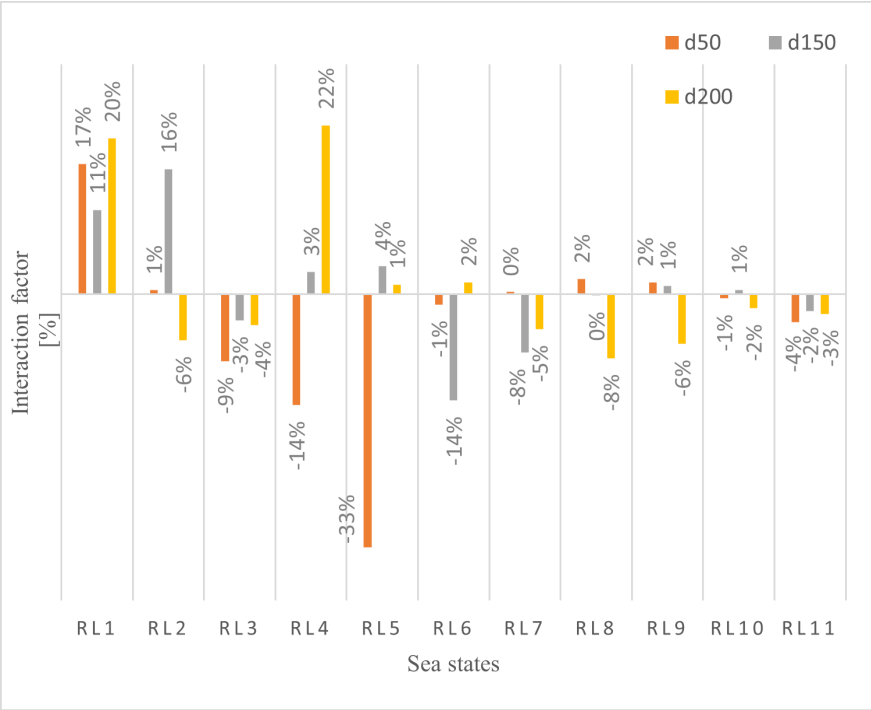

Figure 4-13: Interaction factor for regular low sea state.

4.3.1.2 Regular high

Figure 4-14 shows the comparison between interaction factor for regular high sea state and regular low sea states for 150 m layout. It follows a similar trend as the power analysis Figure 4-8. Even though the regular analysis shows a dip in the power trend due to resonance, the normalization helps in understanding the interaction effects in this range. It is to be noted that the dip in the power trend is not completely reliable as it requires more fine tuning of the PTO system.

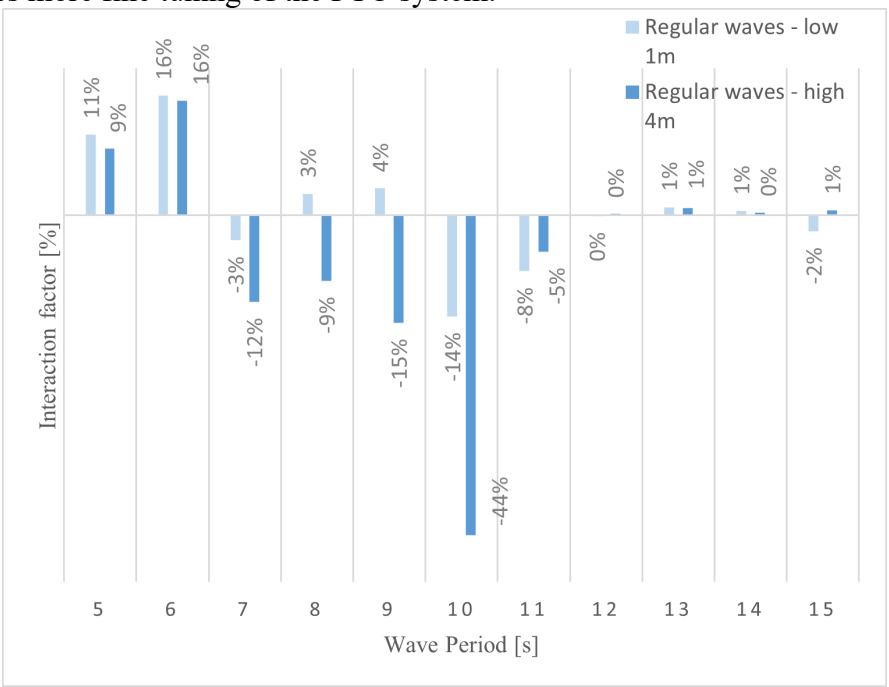

Figure 4-14: Interaction factor for regular low and high sea states for 150 m layout.

4.3.2 Irregular sea state

The power performance of the irregular sea state is assessed under various conditions, using the same methodology as discussed in the regular sea state. The interaction factor for the irregular sea state is observed in Figure 4-15. It is observed that, throughout the sea states, the 200 m WEC array performs marginally better than the 150m WEC array with a better interaction factor. The 50 m WEC distance performs bad in the sea states having *Tp* = 7.5 s.

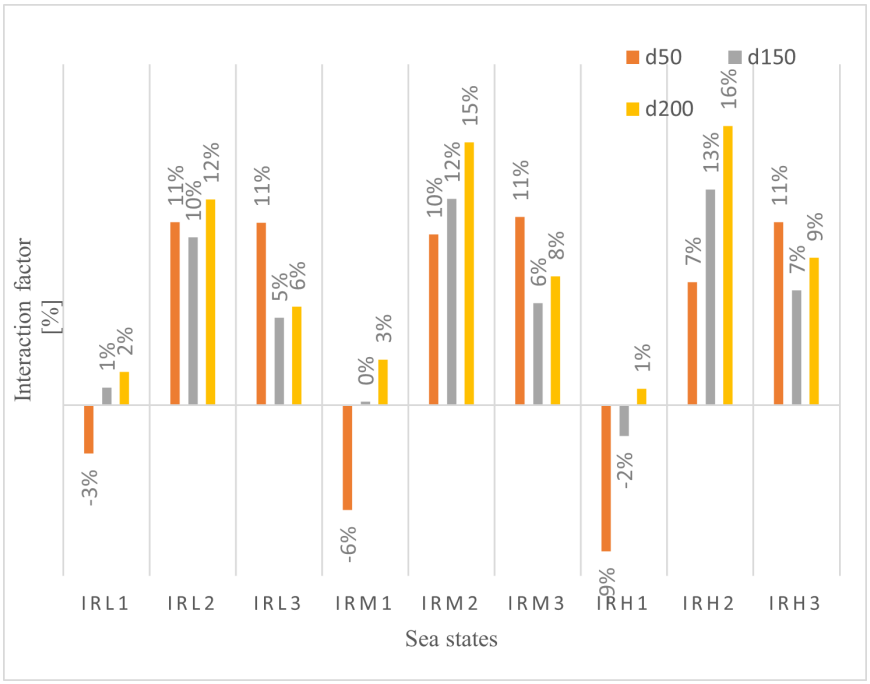

Figure 4-15: Interaction factors for irregular sea states.

4.3.2.1 Water depth influence

In Section 4.2.2.1, the water depth effect on power production was studied and the difference in power between the two water depths 46 m and 55 m was found to be very small. The interaction effects at these two water depths are shown in Figure 4-16. In IRL1 sea state with a significant wave height *Hs* of 1.75 m and peak period *Tp* of 7.5 s, WECs experience very low interaction effects of 1% and 2% compared to the other 2 sea states. This effect is mainly due to the energy of the wave being low at these wave heights. The diffracted and radiated waves from the WECs do not carry enough energy to affect the successive rows of the WEC array. However, at sea state IRL2 even though the *Hs* remains the same as the surge resonance is significantly high at these time period as observed in Section 4.2.1. This suggests that the increase in surge motions of the WEC will create diffracted waves with higher energies that will carry on for the downstream WECs in the array.

In irregular waves most of the interaction between the WECs observed are constructive interactions. This is because of the composition of the irregular waves. Since the wave spectrum has many waves with different wave periods included in them, the chances are that the radiation and diffraction will superpose with an incident wave of similar wave period and generate constructive interaction. Although the same could also be said for the destructive interaction, however, the refracted and diffracted wave amplitudes are much smaller in the grand scale of irregular sea state. Causing destructive interaction and cancelling out one or two components of lower energy waves will not cause significant reduction in the interaction factor.

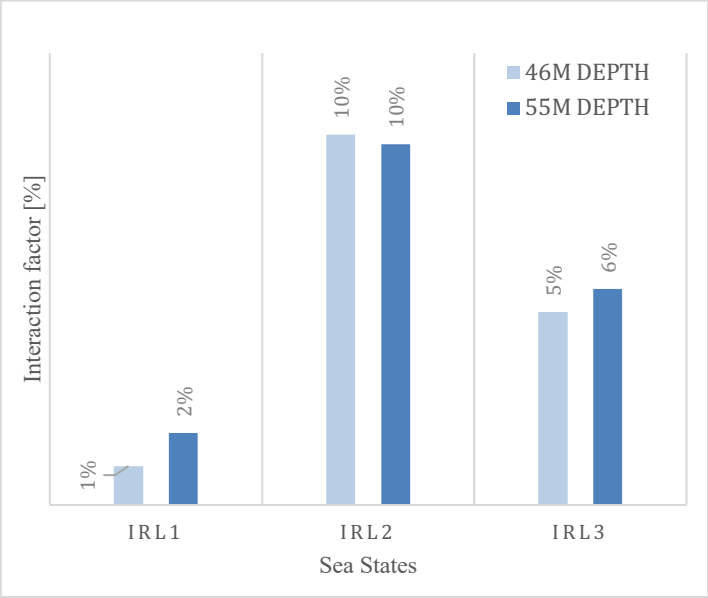

Figure 4-16: Interaction factor for 150m WEC layout at different water depth.

4.3.2.2 Layout influence

The WEC array layout has a significant effect in the interaction between WECs. The arrangement of the WECs can be made in many patterns. In this thesis, 2 patterns were analysed. The square layout and the rectangular layout as described in Section 3.2. The power analysis in Section 4.2.2.2. is indicative of the interaction effects between the WECs in downstream of the layout. In Figure 4-17 it is seen that the 8x2 layout has better interaction factor than the 4x4 layout at sea state IRL1 and for IRL2 and IRL3 the 4x4 layout has better interaction factor.

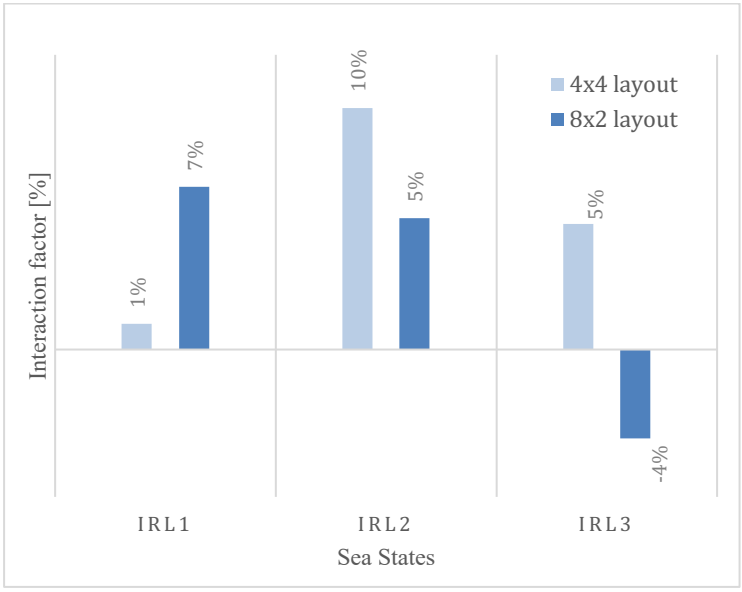

Figure 4-17: Interaction factor for 4x4 and 8x2 layouts in sea states IRL1-3.

The interaction effects observed in Figure 4-17 can be further explained by analysing the individual WEC performance of the two layouts. In Figure 4-18a the interaction effects for the 4x4 layout in the downstream WECs appear to be destructive in comparison with the first row, although it is 1% better than the reference condition, the 8x2 layout performs much better than 4x4 layout the difference in this number is mainly

because the WECs facing the incident wave in 8x2 layout does not experience interaction effects from the downstream WECs and the second row follows the same output but slightly lower than the first row and significantly higher compared to the 2nd, 3rd and 4th rows of the 4x4 layout.

Figure 4-18b shows the interaction effects in the IRL3 sea state. In this analysis the 4x4 layout exhibits a successive interaction at peak period of 11.5 s. It is clear from the figure that most of the downstream WECs in the 4x4 layout i.e., 2nd, 3rd and 4th rows perform better than the WECs facing the incident wave. The 8x2 layout performs similar to IRL1 but the interaction factor is -4%. This indicates that the interaction between the converters is destructive, and it is hindering the power performance. The unevenness of the overall power production across the row of WECs is a result of difference in encountered waves. The principal wave direction is same for all the WECs in the array, but they experience different wave amplitudes since the simulation is carried out using short-crested waves.

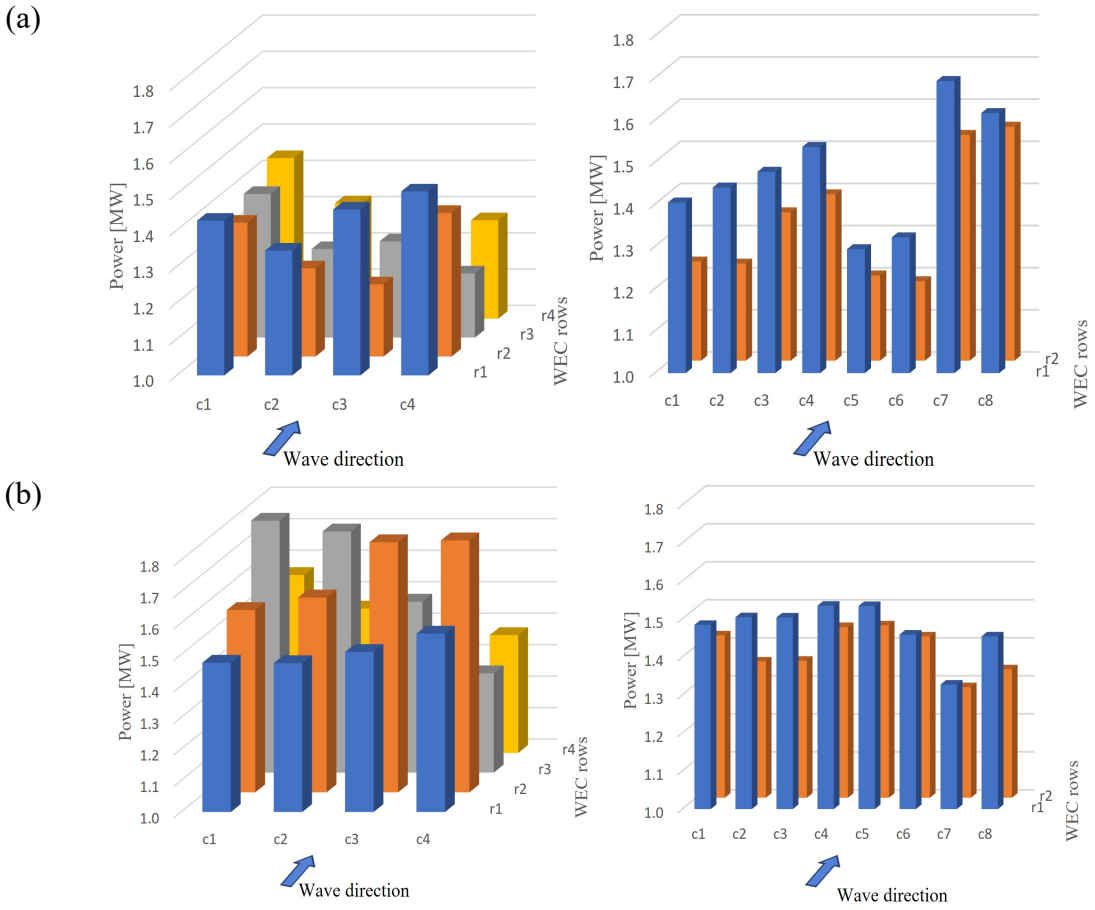

Figure 4-18: Individual WEC power performance in 4x4 layout (left) and 8x2 layout (right) in sea state IRL1(a) and sea state IRL3(b).

4.3.2.3 Wave encounter direction angle influence

Figure 4-19 shows the interaction factor at different incident wave angles. This is also a comparison where the sea state is different for each condition hence the observation must be made in individual sea states. In IRL1 sea state an angle of 4.7º is compared with the 0º incident angle. It is found that the interaction factor increases to 4% from 1% at this angle. As the angle shifts to 9.4º in sea state IRL2, the interaction factor

reduces by 5% indicating that the successive interaction is less than what it is observed at 0º. In IRL3 sea state, however, the angle analysed is 14º and the difference between the two cases is only by a percentage. Even though at 0º the difference between 3 sea states is more visible, it is not so much in the case of angles other than 0º.

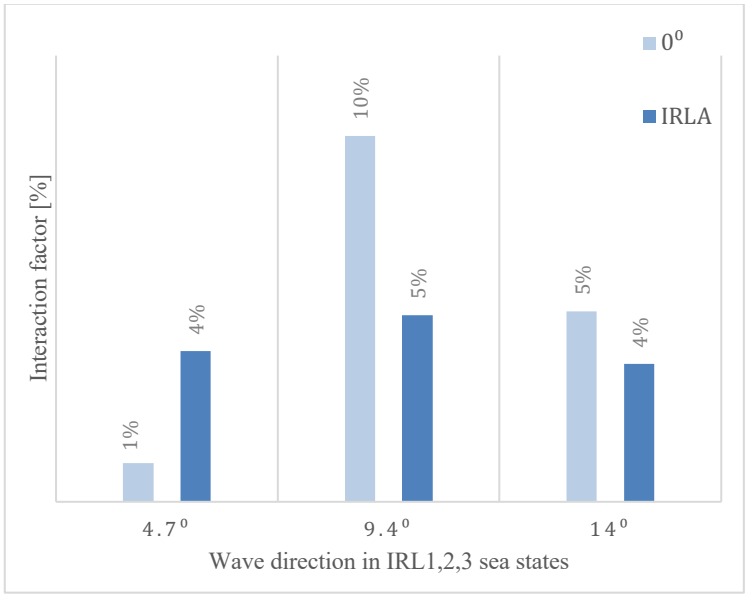

Figure 4-19: Interaction factor for different incident angles for the 4x4 layout for the sea states IRL1-3.

5 Conclusions

The WEC technology holds significant promise as a renewable energy source, even as it continues to undergo research and development. Installations are already underway, marking progress in its application. However, there are crucial aspects that need to be highlighted to comprehensively grasp the technology and unlock its complete potential. This thesis studies interaction effects as a crucial factor using the floating-point absorber WEC technology developed by CorPower. Multiple simulations were conducted to understand and interpret the difference in the behaviour of a single WEC and WECs installed in an array. The environmental conditions i.e., sea states used in this thesis resemble the real sea states observed in most seas together with design parameters such as wave direction, water depth, layout of the WEC array, and the distance between the WEC's in an array.

It was observed in the power analysis that power trend is directly dependent on the energy of the sea state. In the regular sea state, a dip in the power trend was observed near half surge resonance that reduced the heave motions resulting directly in lower power output. This effect is not observed in irregular sea states because of the different encountering wave frequencies that do not allow the WEC to fully resonate.

In the regular seas analysis of 4x4 array layout with three different distance parameters 50 m, 150 m, and 200 m, it was observed that the surge resonance increases the interaction effects by generating more interaction waves. This surge motion affects the heave motion of the WEC and the total power production. For the 50 m WEC distance, 33% destructive interaction was observed in regular low seas and a 44% destructive interaction was observed for 150 m WEC distance in regular high seas. This showed that the energy of the sea state had a bigger impact on the observed interaction effects. However, these effects were not visible in irregular seas since this sea state is made up of waves with different time periods and a single wave component is not prolonged. A maximum of 13% positive interaction effect is observed of 150 m WEC array in the irregular sea state.

It was found that the interaction effects in comparison to the power produced were small and within 15% for the WEC array of 150 m separating distance in irregular sea states. The results do not indicate that an array model performs optimally in all environmental and design conditions. The number of simulations were extensive and the optimal arrangement depends on the limited sea states that the WEC is expected to be installed.

Furthermore, in the water depth study, the difference observed by depth change from 46 m to 55 m is found to be very small in terms of interaction effect as well as power analysis. In irregular seas with the least energy IRL. The interaction effects observed were within 1%. However, this observation showed that the surge resonance of the WEC is not prolonged and does not contribute to destructive interaction as observed in regular sea states.

The interaction effects showed clear differences in all 3 simulated sea states in comparing different layouts. A maximum of 9% interaction effects are seen with the 8x2 WEC array showing destructive interaction of -4% and the 4x4 array with a constructive interaction of 5% in the IRL3 sea state. However, the 8x2 layout performs better in the IRL1 sea state.

It was found that different wave angle increases the interaction by 4% for 4.7º and at 9.4º the interaction effects increase to 5%, whereas, in the same sea state at 0º, a 10% constructive interference is observed.

This study highlights the importance of performing interaction simulation studies for WECs installed in an array. This approach ensures the technology is optimally utilized before deploying a larger physical setup. The methodology followed in this thesis demonstrates how to proceed with the studies regarding the development of larger arrays and not the optimization of the array itself. The interaction factors observed in the study provide a baseline to conduct extensive study by isolating parameters that influence this effect.

It is concluded that the design of wave farms should follow a methodology that incorporates interaction effects in the design stage. Optimization of the arrays will take up a broader part of this study. Establishing a baseline for the interaction factor and conducting further in-depth studies is important.

6 Future work

This chapter suggests some of the future work that would benefit and extend these results. The study specifically introduces the potential factors and examined its effects in detailed for the CorPower CorPack while the run list is specifically designed for this analysis. The thesis addresses the interaction effect and the performance evaluation. The goal is to develop the tool to study and optimise the array further for these interaction effects. This study can be further extended in the following topics:

Different WEC type study

The WEC technology is in the state of constant evolution and there is no perfect solution to harness the wave energy and so there are several concepts developed. This study presents a single type of WEC technology. The INTERACT project investigates two more types of WECs. It is of interest to understand the similarities and differences between WEC technologies and wave park patterns. Therefore, it is important to study in detail how this methodology and parameters have effects on the other types of WECs and their behaviour. The aim is for the tool to be adaptable for diverse characteristics of different WEC types.

PTO model with more control parameters

The PTO model used in this study is not completely optimised for all the environmental loads. The added structural response at mooring is a constant pretension force and this can be developed to have real time control to match the dynamic response of the PTO system. A better system with active control parameters for a broader range of wave forces would add significant changes to the results obtained. Some undesirable effects observed in the power trend can be eliminated.

Simulations with different array layouts

The arrays considered for this study is a square and a rectangular pattern. There are multiple array patterns that are already being evaluated for performance as seen in studies conducted by Yang et al. (2020) and Ringsberg et al. (2020). Although the designs of the WEC system used in this thesis plays an important role to validate the results of some designs. The optimisation can take place through many different software as seen in one of the studies conducted by Garcia-Rosa et al. (2015).

Increasing the range of the water depths

This study acknowledges a limitation in the in-depth exploration of water depth. Originally, the intention was to conduct analyses across a range of water depths. However, due to time constraints and the specific installation site of the CorPower technology, this parameter was limited. The actual application of the technology is focused on a specific water depth, hence the absence of a diverse range of water depth values.

Introduction of biofouling

Biofouling on the power performance was planned in the simulation matrix by increasing the diameter of the buoy. However, due to time constraints, this study has not been carried out. An interesting area of research for the future is investigating how biofouling affects WEC arrays. Yang et al. (2017) showed that biofouling has the potential to affect important factors like power absorption, component durability, and fatigue damage. Examining the relationship between biofouling and WEC performance may offer important insights for improving array effectiveness, maintenance tactics, and system sustainability. Studies that follow to mitigate the effects of biofouling by innovative materials, coatings, or operating strategies will ultimately help wave energy conversion technology remain effective over the long run.

Fatigue analysis of the mooring system and LCoE analysis

Yang (2018) shows the influence of the hydrodynamic and structure response on the fatigue life characteristics of the structures. Examining the influence of environmental loads causing fatigue damage ensures the reliable design of structures. These considerations have been proven to be crucial in the long-term structural integrity and operational reliability of the WEC array. Exploring how the dynamic forces are exerted by waves and their impact on mooring components over time could aid in the development of sustainable systems.

The LCoE analysis will provide an overall perspective of cost effectivity with performance of the WEC technology by considering several factors such as installation, maintenance, operation, and life cycle of the WEC array.

7 References

Aderinto, T. & Li, H. 2019. Review on Power Performance and Efficiency of Wave Energy Converters. *Energies,* 12**,** 4329.

Babarit, A. 2013. On the park effect in arrays of oscillating wave energy converters. *Renewable Energy,* 58, 68-78.

Bombora. 2023. *mwave* [Online]. Available: https://bomborawave.com/mwave/ [Accessed 01-02-2023].

Borgarino, B., Babarit, A. & Ferrant, P. 2012. Impact of wave interactions effects on energy absorption in large arrays of wave energy converters. *Ocean Engineering,* 41**,** 79-88.

Corpower Ocean. 2023. *C4 Wave energy converter* [Online]. CorPower Ocean. Available: https://corpowerocean.com/wave-energy-technology/ [Accessed 01-02-2023].

Czech, B. & Bauer, P. 2012. Wave Energy Converter Concepts : Design Challenges and Classification. *IEEE Industrial Electronics Magazine,* 6**,** 4-16.

Dnv Gl. 2017. *HydroD V4.10* [Online]. Available: https://www.dnv.com/services/sesam-for-marine-systems-modules-2323 [Accessed 01-02-2023].

Dnv Gl. 2019a. *RIFLEX 4.16.2* [Online]. Available: https://www.dnv.com/services/sesam-for-marine-systems-modules-2323 [Accessed 01-02-2023].

Dnv Gl. 2019b. *Sesam software - Strength assessment of offshore structures* [Online]. Available: https://www.dnv.com/software/services/index.html? [Accessed 2023-02-01].

Dnv Gl. 2019c. *SIMO V 4.2.0* [Online]. Available: https://www.dnv.com/services/sesam-for-marine-systems-modules-2323 [Accessed 01-02-2023].

Dnv Gl. 2019d. *Wadam v9.7* [Online]. Available: https://www.dnv.com/services/sesam-for-marine-systems-modules-2323 [Accessed 01-02-2023].

Dnv Gl. 2022. *SIMA* [Online]. Available: https://www.dnv.com/services/sesam-for-marine-systems-modules-2323 [Accessed 1 February 2023].

Drew, B., Plummer, A. R. & Sahinkaya, M. N. 2009. A review of wave energy converter technology. *Proceedings of the Institution of Mechanical Engineers Part a-Journal of Power and Energy,* 223**,** 887-902.

Emec. 2023. *Technology readiness level* [Online]. European Marine Energy Centre. Available: https://www.emec.org.uk/services/provision-of-wave-and-tidal-testing/pathway-to-emec/technology-readiness-levels/ [Accessed 02/05/2023].

Engström, J., Eriksson, M., Göteman, M., Isberg, J. & Leijon, M. 2013. Performance of large arrays of point absorbing direct-driven wave energy converters. *Journal of Applied Physics,* 114.

Eu. 2023. *European Commission - Energy - Topics - Renewable energy* [Online]. Available: https://energy.ec.europa.eu/topics/renewable-energy/renewable-energy-directive-targets-and-rules/renewable-energy-directive_en [Accessed 02/05/2023].

Falcão, A. F. D. O. 2010. Wave energy utilization: A review of the technologies. *Renewable and Sustainable Energy Reviews,* 14**,** 899-918.

Garcia-Rosa, P. B., Bacelli, G. & Ringwood, J. V. 2015. Control-Informed Optimal Array Layout for Wave Farms. *IEEE Transactions on Sustainable Energy,* 6**,** 575-582.

Geps Techno. 2023. *WAVEGEM - Hybrid platform* [Online]. Available: https://geps-techno.com/en/your-applications/offshore-power/ [Accessed 01-02-2023].

Güney, T. 2019. Renewable energy, non-renewable energy and sustainable development. *International Journal of Sustainable Development & World Ecology,* 26**,** 389-397.

Guo, B., Wang, T., Jin, S., Duan, S., Yang, K. & Zhao, Y. 2022. A Review of Point Absorber Wave Energy Converters. *Journal of Marine Science and Engineering,* 10**,** 1534.

Harris, R. E., Johanning, L. & Wolfram, J. 2004. Mooring systems for wave energy converters: A review of design issues and choices. *Marec2004***,** 180-189.

Hasanuzzaman, M., Islam, M. A., Rahim, N. A. & Yanping, Y. 2020. Chapter 3 - Energy demand. *In:* HASANUZZAMAN, M. D. & RAHIM, N. A. (eds.) *Energy for Sustainable Development.* Academic Press.

Interact Project. 2020. *INTERACT - Analysis of array systems of wave energy converters with regard to interaction effects in the LCOE and fatigue analyses* [Online]. Available: https://research.chalmers.se/en/project/?id=9743 [Accessed 2023-02-01].

Mathworks. 2021. *MATLAB R2021a* [Online]. Available: https://se.mathworks.com/products/matlab.html [Accessed 01-02-2023].

Polinder, H. & Scuotto, M. Wave energy converters and their impact on power systems. 2005 International Conference on Future Power Systems, 2005-01-01 2005. IEEE.

Previsic, M. 2005. Wave power technologies *IEEE Power Engineering Society General Meeting,* 2**,** 2011-2016

Ringsberg, J. W., Jansson, H., Örgård, M., Yang, S.-H. & Johnson, E. 2020. Design of Mooring Solutions and Array Systems for Point Absorbing Wave Energy Devices—Methodology and Application. *Journal of Offshore Mechanics and Arctic Engineering,* 142.

Ruehl, K., Bull, D. & Ieee. 2012. Wave Energy Development Roadmap: Design to Commercialization. MTS/IEEE Oceans Conference, Oct 14-19 2012 Virginia Beach, VA.

Sasaki, W. 2017. Predictability of global offshore wind and wave power. *International Journal of Marine Energy,* 17**,** 98-109.

Sinha, A., Karmakar, D. & Guedes Soares, C. 2016. Performance of optimally tuned arrays of heaving point absorbers. *Renewable Energy,* 92**,** 517-531.

Wave Dragon. 2023. *Wave Dragon over topping device* [Online]. Available: https://wavedragon.net/ [Accessed 01-02-2023].

Waves4power. 2023. *Wave EL the converter* [Online]. Available: https://www.waves4power.com/ [Accessed 01-02-2023].

Yang, S.-H. 2018. *Analysis of the fatigue characteristics of mooring lines and power cables for floating wave energy converters.* Ph.D. thesis, Chalmers University of Technology, Gothenburg, Sweden.

Yang, S.-H., Ringsberg, J. W. & Johnson, E. 2020. Wave energy converters in array configurations—Influence of interaction effects on the power performance and fatigue of mooring lines. *Ocean Engineering,* 211.

Yang, S. H., Ringsberg, J. W., Johnson, E. & Hu, Z. Q. 2017. Biofouling on mooring lines and power cables used in wave energy converter systems-Analysis of fatigue life and energy performance. *Applied Ocean Research,* 65**,** 166-177.

Yang, S. H., Ringsberg, J. W., Johnson, E., Hu, Z. Q. & Palm, J. 2016. A comparison of coupled and de-coupled simulation procedures for the fatigue analysis of wave energy converter mooring lines. *Ocean Engineering,* 117**,** 332-345.

8 Appendix

8.1 Power output for all simulations

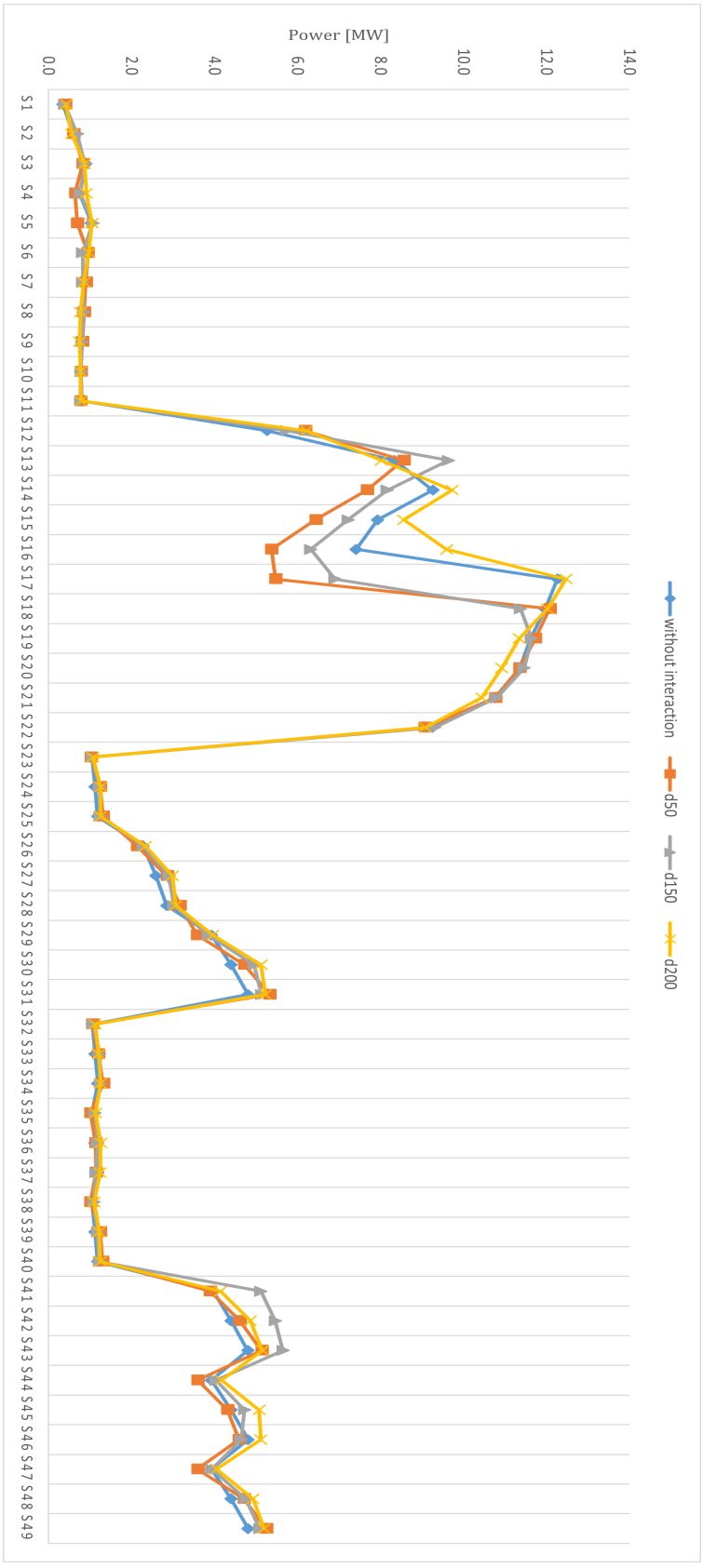

Figure 8-1: Power Analysis results.

Table 8-1: Power produced for all simulations [MW].

	Sea States	without interaction	d50	d150	d200
Regular waves - low 1m	RL1	0.4	0.4	0.4	0.4
	RL2	0.6	0.6	0.7	0.6
	RL3	0.9	0.8	0.9	0.9
	RL4	0.8	0.6	0.8	0.9
	RL5	1.0	0.7	1.1	1.1
	RL6	1.0	0.9	0.8	1.0
	RL7	0.9	0.9	0.8	0.9
	RL8	0.8	0.9	0.8	0.8
	RL9	0.8	0.8	0.8	0.7
	RL10	0.8	0.8	0.8	0.8
	RL11	0.8	0.8	0.8	0.8
Regular waves - high 4m	RH1	5.3	6.2	5.8	6.2
	RH2	8.3	8.6	9.6	8.0
	RH3	9.3	7.7	8.2	9.7
	RH4	7.9	6.4	7.2	8.6
	RH5	7.4	5.4	6.3	9.6
	RH6	12.3	5.5	6.9	12.5
	RH7	12.0	12.1	11.4	12.0
	RH8	11.6	11.7	11.6	11.3
	RH9	11.4	11.4	11.5	10.9
	RH10	10.8	10.8	10.8	10.4
	RH11	9.3	9.1	9.3	9.1
Irregular waves 46M DEPTH 4x4 layout 0º	IRL1	1.1	1.0	1.1	1.1
	IRL2	1.1	1.2	1.2	1.3
	IRL3	1.2	1.3	1.2	1.3
	IRM1	2.3	2.1	2.3	2.3
	IRM2	2.6	2.9	2.9	3.0
	IRM3	2.9	3.2	3.0	3.1
	IRH1	3.9	3.6	3.9	4.0
	IRH2	4.4	4.7	5.0	5.1
	IRH3	4.8	5.3	5.1	5.2
Depth influence 55M DEPTH	IRLW1	1.1	1.1	1.1	1.1
	IRLW2	1.1	1.2	1.2	1.2
	IRLW3	1.2	1.3	1.3	1.3
Layout influence 8x2 layout	IRLL1	1.1	1.0	1.1	1.1
	IRLL2	1.1	1.1	1.2	1.3
	IRLL3	1.2	1.2	1.1	1.2
Angle influence	IRLA1	1.1	1.0	1.1	1.1
	IRLA2	1.1	1.2	1.2	1.2
	IRLA3	1.2	1.3	1.2	1.3
Depth influence	IRHW1	4.0	3.9	5.1	4.1
	IRHW2	4.4	4.6	5.5	4.9
	IRHW3	4.8	5.1	5.7	5.2
Layout influence	IRHL1	3.9	3.6	4.0	4.2
	IRHL2	4.4	4.3	4.7	5.1
	IRHL3	4.8	4.6	4.6	5.1
Angle influence	IRHA1	3.9	3.6	3.9	4.1
	IRHA2	4.4	4.7	4.8	4.9
	IRHA3	4.8	5.2	5.1	5.2

8.2 Interaction analysis for all simulations

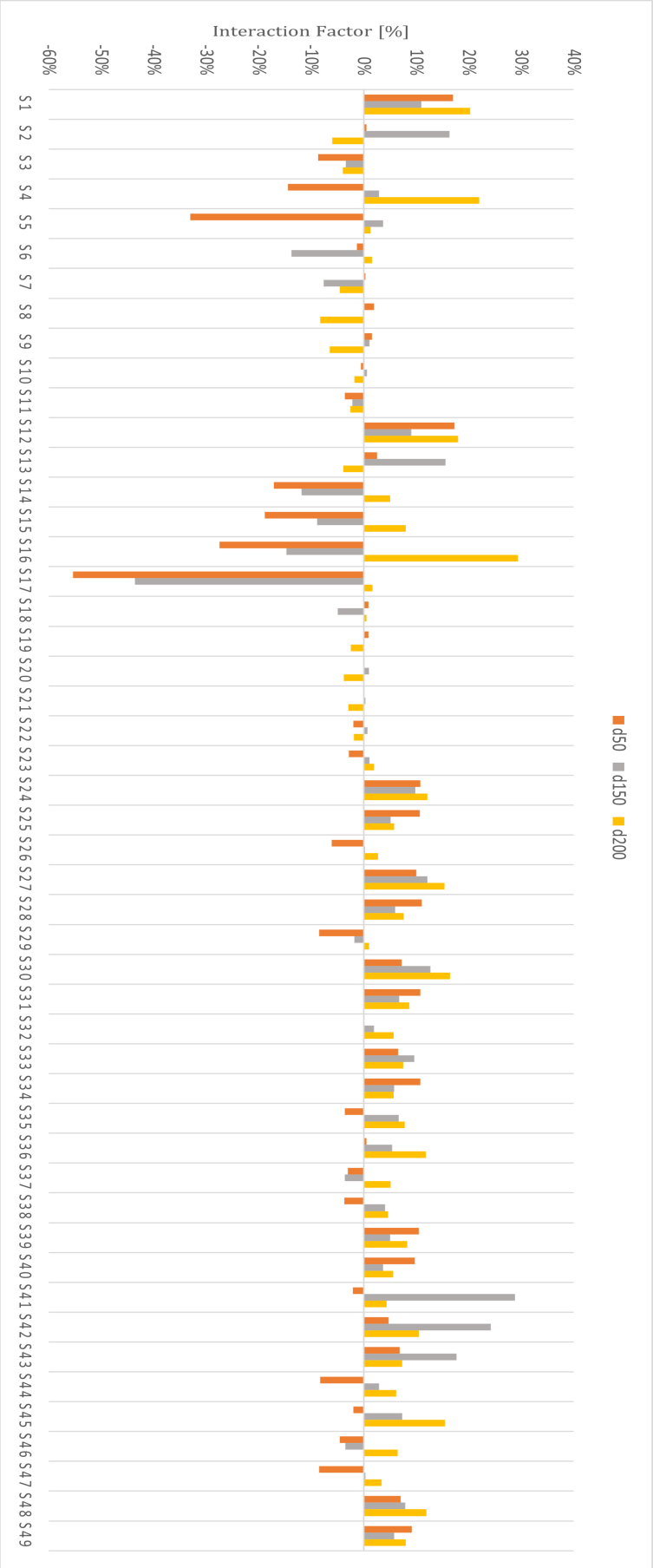

Figure 8-2: Interaction factor.

Table 8-2: Interaction factor.

	Sea States	without interaction Power [MW]	d50	d150	d200
Regular waves - low 1m	RL1	0.4	17%	11%	20%
	RL2	0.6	1%	16%	-6%
	RL3	0.9	-9%	-3%	-4%
	RL4	0.8	-14%	3%	22%
	RL5	1.0	-33%	4%	1%
	RL6	1.0	-1%	-14%	2%
	RL7	0.9	0%	-8%	-5%
	RL8	0.8	2%	0%	-8%
	RL9	0.8	2%	1%	-6%
	RL10	0.8	-1%	1%	-2%
	RL11	0.8	-4%	-2%	-3%
Regular waves - high 4m	RH1	5.3	17%	9%	18%
	RH2	8.3	3%	16%	-4%
	RH3	9.3	-17%	-12%	5%
	RH4	7.9	-19%	-9%	8%
	RH5	7.4	-28%	-15%	29%
	RH6	12.3	-55%	-44%	2%
	RH7	12.0	1%	-5%	0%
	RH8	11.6	1%	0%	-2%
	RH9	11.4	0%	1%	-4%
	RH10	10.8	0%	0%	-3%
	RH11	9.3	-2%	1%	-2%
Irregular waves 46M DEPTH 4x4 layout 0º	IRL1	1.1	-3%	1%	2%
	IRL2	1.1	11%	10%	12%
	IRL3	1.2	11%	5%	6%
	IRM1	2.3	-6%	0%	3%
	IRM2	2.6	10%	12%	15%
	IRM3	2.9	11%	6%	8%
	IRH1	3.9	-9%	-2%	1%
	IRH2	4.4	7%	13%	16%
	IRH3	4.8	11%	7%	9%
Depth influence 55M DEPTH	IRLW1	1.1	0%	2%	6%
	IRLW2	1.1	7%	10%	8%
	IRLW3	1.2	11%	6%	6%
Layout influence 8x2 layout	IRLL1	1.1	-4%	7%	8%
	IRLL2	1.1	0%	5%	12%
	IRLL3	1.2	-3%	-4%	5%
Angle influence	IRLA1	1.1	-4%	4%	5%
	IRLA2	1.1	10%	5%	8%
	IRLA3	1.2	10%	4%	6%
Depth influence	IRHW1	4.0	-2%	29%	4%
	IRHW2	4.4	5%	24%	10%
	IRHW3	4.8	7%	18%	7%
Layout influence	IRHL1	3.9	-8%	3%	6%
	IRHL2	4.4	-2%	7%	15%
	IRHL3	4.8	-5%	-3%	6%
Angle influence	IRHA1	3.9	-8%	0%	3%
	IRHA2	4.4	7%	8%	12%
	IRHA3	4.8	9%	6%	8%

8.3 Normalized Power

Table 8-3: Normalized power in each condition set.

	Sea States	without interaction Power [MW]	d50	d150	d200
Regular waves - low 1m	RL1	0.00	0.00	0.00	0.00
	RL2	0.36	0.36	0.45	0.23
	RL3	0.81	0.77	0.71	0.71
	RL4	0.58	0.43	0.56	0.79
	RL5	1.00	0.53	1.00	1.00
	RL6	0.89	1.00	0.64	0.88
	RL7	0.79	0.91	0.64	0.69
	RL8	0.72	0.84	0.66	0.56
	RL9	0.65	0.75	0.61	0.52
	RL10	0.63	0.69	0.58	0.55
	RL11	0.65	0.67	0.57	0.57
Regular waves - high 4m	RH1	0.00	0.12	0.00	0.00
	RH2	0.44	0.47	0.66	0.29
	RH3	0.57	0.34	0.41	0.56
	RH4	0.38	0.16	0.25	0.37
	RH5	0.31	0.00	0.10	0.54
	RH6	1.00	0.01	0.20	1.00
	RH7	0.96	1.00	0.96	0.93
	RH8	0.91	0.95	1.00	0.82
	RH9	0.87	0.89	0.97	0.75
	RH10	0.79	0.81	0.86	0.68
	RH11	0.57	0.55	0.60	0.46
Irregular waves 46M DEPTH 4x4 layout 0^{o}	IRL1	0.00	0.00	0.00	0.00
	IRL2	0.56	0.78	0.95	1.00
	IRL3	1.00	1.00	1.00	0.96
	IRM1	0.00	0.00	0.00	0.00
	IRM2	0.54	0.69	0.84	0.89
	IRM3	1.00	1.00	1.00	1.00
	IRH1	0.00	0.00	0.00	0.00
	IRH2	0.54	0.65	0.86	0.92
	IRH3	1.00	1.00	1.00	1.00
Depth influence 55M DEPTH	IRLW1	0.00	0.00	0.00	0.00
	IRLW2	0.51	0.55	0.87	0.67
	IRLW3	1.00	1.00	1.00	1.00
Layout influence 8x2 layout	IRLL1	0.00	0.00	0.00	0.00
	IRLL2	0.56	0.87	1.00	1.00
	IRLL3	1.00	1.00	0.33	0.89
Angle influence	IRLA1	0.00	0.00	0.00	0.00
	IRLA2	0.56	0.81	0.66	0.78
	IRLA3	1.00	1.00	1.00	1.00
Depth influence	IRHW1	0.00	0.00	0.00	0.00
	IRHW2	0.52	0.58	0.65	0.71
	IRHW3	1.00	1.00	1.00	1.00
Layout influence	IRHL1	0.00	0.00	0.00	0.00
	IRHL2	0.54	0.72	1.00	0.96
	IRHL3	1.00	1.00	0.88	1.00
Angle influence	IRHA1	0.00	0.00	0.00	0.00
	IRHA2	0.54	0.68	0.71	0.77
	IRHA3	1.00	1.00	1.00	1.00

8.4 MATLAB code for post processing

```
clc
clear
%% DAMPING
damping = readmatrix('directory\usefuldamping.xlsx','Range','A1:B49'); % path is directory
sim_no = damping(:,1);
pto_losses = 0;
usefuldamping = pto_losses+damping(:,2);


%%

runsection = input('Do you want to run reference simulations? \n(y/n): ', 's');

if strcmpi(runsection, 'y')

    disp(' running reference cases');

      %%load EXCEL to STRUCT for simulations without interaction i.e, REFERENCE
      run directory\ref\ref.m

      %% generate variables
      ref=genvarname(repmat({'ref'},49,1),'ref');
      wec_pto_ref=genvarname(repmat({'wec_pto_ref'},49,1),'wec_pto_ref');
      Tr = zeros(1,numel(ref));
      power_take_out_ref = zeros(numel(ref),1);
      wecs_total_velocity_ref=0;

      %referece case
      for j=1:numel(ref)
          %time
          %Tr(j) = max(allref.(ref{j}).time)-min(allref.(ref{j}).time);

          % reference cases
          wecs_total_velocity_ref = sum(allref.(ref{j}).heave_velocity_sq,2,'omitnan')*16;
          wec_pto_ref{j} = (usefuldamping(j)*wecs_total_velocity_ref')/numel(allref.(ref{j}).time);
          power_take_out_ref(j,1) = power_take_out_ref(j,1) +  sum(wec_pto_ref{j});
      end
      writematrix(power_take_out_ref,'simulation_matrix.xlsx','Sheet',1,'Range','F6:F54')
%reference cases

   else
     disp('reference simulations skipped.');

end


%% load EXCEL to STRUCT for simulations with interaction SIM
runsection = input('Do you want to run all simulations for one layout? \n(y/n): ', 's');

if strcmpi(runsection, 'y')

      validInput = false;
      while ~validInput

         layout = input('Enter a valid layout distance\n(50, 150, or 200): ');

         if layout == 50 || layout == 150 || layout == 200
            validInput = true;
```

```
        else
            disp('Invalid input. Please try again.');
        end
    end

    disp(['Valid input received: ', num2str(layout)]);

    if layout == 50
        disp('running Layout 50m.');
        run directory\d50\d50.m
    else if layout == 150
            disp('running Layout 150m.');
            run directory\d150\d150.m
        else if layout == 200
                disp('running Layout 200m.');
                run directory\d200\d200.m
            else
                disp('Enter a valid layout distance');
            end
        end
    end

    %% generate variables
    sim=genvarname(repmat({'sim'},49,1),'sim');
    wec_pto=genvarname(repmat({'wec_pto'},49,1),'wec_pto');
    Ts = zeros(1,numel(sim));
    power_take_out = zeros(numel(sim),1);

    wecs_total_velocity=0;

    % simulation
    for k=1:numel(sim)
        % time
        Ts(k) = max(allsim.(sim{k}).time)-min(allsim.(sim{k}).time);

        % simulations
        wecs_total_velocity = sum(allsim.(sim{k}).heave_velocity_sq,2,'omitnan');
%single wecs velocity sum
        wec_pto{k} = (usefuldamping(k)*wecs_total_velocity')/numel(allsim.(sim{k}).time);
%single wecs power in Watt
        power_take_out(k,1) = power_take_out(k,1) +  sum(wec_pto{k});
    end
    if layout == 50
        disp('write Layout 50m.');
        writematrix(power_take_out,'simulation_matrix.xlsx','Sheet',1,'Range','G6:G54')     %50m
layout
    else if layout == 150
            disp('write Layout 150m.');
            writematrix(power_take_out,'simulation_matrix.xlsx','Sheet',1,'Range','H6:H54')
        else if layout == 200
                disp('write Layout 200m.');
                writematrix(power_take_out,'simulation_matrix.xlsx','Sheet',1,'Range','I6:I54')
            end
        end
    end

else
   disp('simulations skipped.');
end
```

```
%% normalisation

% normalized_pto=0;
% for k = 1:49
% normalized_pto(k,1) = ((power_take_out(k)-power_take_out_ref(k))/power_take_out_ref(k));
% end

%% Individual sim

runsection = input('Do you want to run power take out for numbered simulations? \n(y/n): ', 's');
   if strcmpi(runsection, 'y')

     simno = false;
     while ~simno

        n = input('Enter a valid simulation number \n(ctrl+c to break the loop): ');
        range = sprintf('A%d:P%d',n,n);
        writecell(wec_pto(n),'WEC_power.xlsx','Sheet',1,'Range',range)

     end


%        sim=genvarname(repmat({'sim'},49,1),'sim');
%        wec_pto=genvarname(repmat({'wec_pto'},49,1),'wec_pto');
%        Ts = zeros(1,numel(sim));
%        power_take_out = zeros(numel(sim),1);
%
%        wecs_total_velocity=0;
%
%        % simulation
%        for k=1:numel(sim)
%           % time
%           Ts(k) = max(allsim.(sim{k}).time)-min(allsim.(sim{k}).time);
%
%           % simulations
%           wecs_total_velocity = sum(allsim.(sim{k}).heave_velocity_sq,2,'omitnan');
%single wecs velocity sum
%           wec_pto{k} = (usefuldamping(k)*wecs_total_velocity')/Ts(k);                %single wecs
power in Watt
%           power_take_out(k,1) = power_take_out(k,1) +  sum(wec_pto{k});
%        end
%        if layout == 50
%           disp('write Layout 50m.');
%           writematrix(power_take_out,'simulation_matrix.xlsx','Sheet',1,'Range','G6:G54')
%50m layout
%        else if layout == 150
%              disp('write Layout 150m.');
%              writematrix(power_take_out,'simulation_matrix.xlsx','Sheet',1,'Range','H6:H54')
%           else if layout == 200
%                 disp('write Layout 200m.');
%                 writematrix(power_take_out,'simulation_matrix.xlsx','Sheet',1,'Range','I6:I54')
%              end
%           end
%        end
%
%
```

```
    else
        disp('End.');
    end

% %
% x = [sim_no(1:11) sim_no(12:22)]
% y = [1*ones(11,1) 2*ones(11,1)]
%
% %[X,Y] = meshgrid(-100:1:100);
% z = [normalized_pto(1:11) normalized_pto(12:22)]
% plot(x,z)
%%%%%%%%%%%%%%%%%%%%%%%%%%%%%%%%%%%%%%%%%%%%%%%%%%%%%%%%%%%%%%%%%%%%%%%%%%%%%%%%%%%%
%%%%%%%%%%%%%%%%%%%%%%%%%%%%
```

8.4.1 MATLAB code for data extraction from directories and dependencies for the main code

For layout 150 data extraction

```
%READ EXCEL FILES for 150m

s = zeros(17,16383);

for n=1:49
    filename = sprintf('s%d.xlsx',n)
    s = xlsread(filename);
    structname = sprintf('sim%d',n);
    allsim.(structname) = struct('time',s(1,:),'heave_velocity_sq',s(2:17,:));
end
clear s
%%%%%%%%%%%%%%%%%%%%%%%%%%%%%%%%%%%%%%%%%%%%%%%%%%%%%%%%%%%%%%%%%%%%%%%%%%%%%%%%%%%%
%%%%%%%%%%%%%%%%%%%%%%%%%%%%%%
```

8.4.2 MATLAB code for Free decay test

```
clc
clear all

%% HEAVE

heave = readmatrix('heavefd.csv');
time = 0:0.05:0+(numel(heave)-1)*0.05;
%time = linspace(0,1000,numel(heave));
%heave=vertcat(heave,time);

heave=heave(5900:7000);
time=time(5900:7000);
%h(2,:)=h(2,:)-600;
%heave=-heave;

[peaksh, peak_indicesh] = findpeaks(heave);

time_differencesh = diff(time(peak_indicesh(2:end)));
resonance_time_periodh = mean(time_differencesh);
disp(['Heave Resonance Time Period: ' num2str(resonance_time_periodh) ' seconds']);

figure
plot(time,heave,'lineWidth',2)
```

```
hold on;
plot(time(peak_indicesh(2:4)), peaksh(2:4), 'r*', 'MarkerSize', 8);
for i = 2:4
    text(time(peak_indicesh(i)), peaksh(i), sprintf('%0.1f', time(peak_indicesh(i))), ...
        'VerticalAlignment', 'bottom', 'HorizontalAlignment', 'center');
end
hold off;


handle=gca;
set(handle,'fontsize',13);
set (gcf,'Position',[100,100,800,600], 'color','w')
xlabel('Time [s]','fontsize',20,'interpreter', 'latex')
ylabel('Heave [m]','fontsize',20,'interpreter', 'latex')
legend('time series data', 'Identified peaks');


%% SURGE
surge = readmatrix('surgefd.csv');
times = 0:0.05:0+(numel(surge)-1)*0.1;
%surge=vertcat(surge,times);

surge=surge(19000:35000);
times = times(19000:35000);

%s(2,:)=s(2,:)-2000;
[peaks, peak_indices] = findpeaks(surge);

time_differences = diff(times(peak_indices(5:end)));
resonance_time_period = mean(time_differences(1:3));
disp(['Surge Resonance Time Period: ' num2str(resonance_time_period) ' seconds']);

figure
plot(times,surge,'lineWidth',2)
hold on;
plot(times(peak_indices(5:7)), peaks(5:7), 'r*', 'MarkerSize', 8);
for i = 5:7
    text(times(peak_indices(i)), peaks(i), sprintf('%0.1f', times(peak_indices(i))), ...
        'VerticalAlignment', 'bottom', 'HorizontalAlignment', 'left');
end
hold off;

handle=gca;
set(handle,'fontsize',13);
set (gcf,'Position',[100,100,800,600], 'color','w')
xlabel('Time [s]','fontsize',20,'interpreter', 'latex')
ylabel('Surge [m]','fontsize',20,'interpreter', 'latex')
legend('time series data', 'Identified peaks');



clear all

%% HEAVE

heave = readmatrix('heavefd.csv');
time = 0:0.05:0+(numel(heave)-1)*0.05;
%time = linspace(0,1000,numel(heave));
%heave=vertcat(heave,time);
```

```
heave=heave(5900:7000);
time=time(5900:7000);
%h(2,:)=h(2,:)-600;
%heave=-heave;

[peaksh, peak_indicesh] = findpeaks(heave);

time_differencesh = diff(time(peak_indicesh(2:end)));
resonance_time_periodh = mean(time_differencesh);
disp(['Heave Resonance Time Period: ' num2str(resonance_time_periodh) ' seconds']);

figure
plot(time,heave,'lineWidth',2)
hold on;
plot(time(peak_indicesh(2:4)), peaksh(2:4), 'r*', 'MarkerSize', 8);
for i = 2:4
   text(time(peak_indicesh(i)), peaksh(i), sprintf('%0.1f', time(peak_indicesh(i))), ...
      'VerticalAlignment', 'bottom', 'HorizontalAlignment', 'center');
end
hold off;


handle=gca;
set(handle,'fontsize',13);
set (gcf,'Position',[100,100,800,600], 'color','w')
xlabel('Time [s]','fontsize',20,'interpreter', 'latex')
ylabel('Heave [m]','fontsize',20,'interpreter', 'latex')
legend('time series data', 'Identified peaks');


%% SURGE
surge = readmatrix('surgefd.csv');
times = 0:0.05:0+(numel(surge)-1)*0.1;
%surge=vertcat(surge,times);

surge=surge(19000:35000);
times = times(19000:35000);

%s(2,:)=s(2,:)-2000;
[peaks, peak_indices] = findpeaks(surge);

time_differences = diff(times(peak_indices(5:end)));
resonance_time_period = mean(time_differences(1:3));
disp(['Surge Resonance Time Period: ' num2str(resonance_time_period) ' seconds']);

figure
plot(times,surge,'lineWidth',2)
hold on;
plot(times(peak_indices(5:7)), peaks(5:7), 'r*', 'MarkerSize', 8);
for i = 5:7
   text(times(peak_indices(i)), peaks(i), sprintf('%0.1f', times(peak_indices(i))), ...
      'VerticalAlignment', 'bottom', 'HorizontalAlignment', 'left');
end
hold off;

handle=gca;
set(handle,'fontsize',13);
set (gcf,'Position',[100,100,800,600], 'color','w')
xlabel('Time [s]','fontsize',20,'interpreter', 'latex')
ylabel('Surge [m]','fontsize',20,'interpreter', 'latex')
```

```
legend('time series data', 'Identified peaks');

%%%%%%%%%%%%%%%%%%%%%%%%%%%%%%%%%%%%%%%%%%%%%%%%
%%%%%%%%%%%%%%%%%%
```

DEPARTMENT OF MECHANICS AND MARITIME SCIENCES
CHALMERS UNIVERSITY OF TECHNOLOGY
Gothenburg, Sweden 2023
www.chalmers.se

CHALMERS
UNIVERSITY OF TECHNOLOGY